

Poster | Material, processing, and characterization

📅 Mon. Jul 28, 2025 4:30 PM - 6:00 PM JST | Mon. Jul 28, 2025 7:30 AM - 9:00 AM UTC 🏠 Yellow zone, Conference rooms 101 and 102(1F)

## **[P1] Processing, Characterization & Thin Films**

Session Chair: Dr. Imants Dirba (Technical University of Darmstadt, Germany), Dr. Tae-Hoon Kim (Korea Institute of Materials Science, Korea)

[P1-50]

Optimization of Processing Parameters for High-Performance Anisotropic Bonded Magnets

\*Ikenna C. Nlebedim<sup>1</sup>, Xubo Liu<sup>1</sup>, Parans Paranthaman<sup>2</sup> (1. Division of Critical Materials, Ames National Laboratory (United States of America), 2. Chemical Sciences Division, Oak Ridge National Laboratory (United States of America))

[P1-51]

Demagnetization Processes in Nd-Fe-B sintered and Ferrite Magnets derived from magnetic measurement and soft X-ray magnetic circular dichroism microscopy

\*Yutaka Matsuura<sup>1</sup> (1. Research Institute for Applied Sciences (Japan))

[P1-52]

Anisotropy field measurement in hard magnets: evaluating current methodologies

\*Alex Aubert<sup>1</sup>, Konstantin Skokov<sup>1</sup>, Oliver Gutfleisch<sup>1</sup> (1. Functional Materials, TU Darmstadt (Germany))

[P1-53]

Angular Dependence of Coercivity and Flux Loss under Tilted Field in Nd-Fe-B Sintered Magnet

\*Hitoshi Yamamoto<sup>1</sup>, Hirotohi Fukunaga<sup>2</sup> (1. Neoji-consul (Japan), 2. Nagasaki University (Japan))

[P1-54]

Pulsed Field Magnetometers - validating data generated by Self-Demagnetisation Field Function (SDFF) correction to create closed loop results from open loop measurements

\*Robin Cornelius<sup>1</sup>, Jian He<sup>2</sup>, Jack Wade<sup>1</sup>, Stuart Harwin<sup>1</sup>, James Mckenzie<sup>1</sup> (1. Hirst Magnetic Instruments Ltd (UK), 2. National Institute of Metrology (China))

[P1-55]

Measuring initial curves and minor hysteresis loops for rare earth magnets using the Pulsed Field Magnetometer (PFM) system

\*Robin Cornelius<sup>1</sup>, Jack Wade<sup>1</sup>, Stuart Harwin<sup>1</sup>, James Mckenzie<sup>1</sup> (1. Hirst Magnetic Instruments Ltd (UK))

[P1-56]

Spectroscopic insights into the electronic structure of non-critical rare earth containing permanent magnets

\*Benedikt Eggert<sup>1</sup>, Alex Aubert<sup>2</sup>, Philipp Kläßen<sup>1</sup>, Janosch Tasto<sup>1</sup>, Nathan Yutronkie<sup>3</sup>, Fabrice Wilhelm<sup>3</sup>, Andrei Rogalev<sup>3</sup>, Konstantin Skokov<sup>2</sup>, Heiko Wende<sup>1</sup>, Oliver Gutfleisch<sup>2</sup>, Katharina Ollefs<sup>1</sup> (1. University of Duisburg-Essen (Germany), 2. Technical University of Darmstadt (Germany), 3. European Synchrotron Radiation Facility (France))

[P1-57]

### Three-dimensional magnetic domain propagation of a Nd-Fe-B hot-deformed magnet

\*Tomomi Suwa<sup>1</sup>, Motohiro Suzuki<sup>2</sup>, Tadakatsu Ohkubo<sup>3</sup>, Iriyama Takahiko<sup>4</sup>, Hiroshi Miyawaki<sup>4</sup>, Kaiki Takemura<sup>2</sup>, Yusuke Akiyama<sup>2</sup>, Takuya Taniguchi<sup>1</sup>, Satoshi Okamoto<sup>1,3</sup> (1. Tohoku University (Japan), 2. Kwansei Gakuin University (Japan), 3. National Institute for Materials Science (Japan), 4. Daido Steel Company, Limited (Japan))

---

[P1-58]

### A New Perspective on Assessing the Magnetic Texture in Nd-Fe-B Magnets: The influence of coercivity

Luis Torres Quispe<sup>1</sup>, \*Wagner Costa Macedo<sup>1</sup>, Marcelo Augusto Rosa<sup>1</sup>, Leonardo Antunes<sup>1</sup>, Apuniano Baldárrago-Alcántara<sup>1</sup>, Paulo Wendhausen<sup>1</sup> (1. Federal University of Santa Catarina (Brazil))

---

[P1-59]

### Temperature field variations during directional solidification of rare-earth large-size Tb-Dy-Fe magnetostrictive materials and their effect on growth orientation

\*Jiang ping xin<sup>1</sup>, Jiheng Li<sup>1</sup>, Xiaoqian Bao<sup>1</sup>, Xuexu Gao<sup>1</sup> (1. USTB (China))

---

[P1-60]

### Bioinspired Design, Fabrication, and Wing Morphing of 3D-Printed Magnetic Butterflies

Muhammad Bilal Khan<sup>1</sup>, Kilan Schäfer<sup>1</sup>, Florian Hofmann<sup>1</sup>, Matthias Lutzi<sup>1</sup>, Eduardo Sergio Oliveros-Mata<sup>2</sup>, Oleksandr Pylypovskyi<sup>2</sup>, Denys Makarov<sup>2</sup>, \*Oliver Gutfleisch<sup>1</sup> (1. Functional Materials, TU Darmstadt (Germany), 2. Institute of Ion Beam Physics and Materials Research Helmholtz-Zentrum Dresden-Rossendorf e.V. (Germany))

---

[P1-61]

### Phase composition and magnetic properties of Nd(Pr)<sub>2</sub>Fe<sub>14</sub>B and (Sm,Zr)Fe<sub>11</sub>Ti magnets produced by selective laser melting

Sergey Andreev<sup>1</sup>, \*Viktoria Maltseva<sup>1</sup>, Dmitriy Neznakhin<sup>1</sup>, Arkadiy Shalaginov<sup>1</sup>, Andrey Urzhumtsev<sup>1</sup>, Alexey Volegov<sup>1</sup> (1. Ural Federal University (Russia))

---

[P1-62]

### Grain alignment by single track printing using anisotropic sintered Nd-Fe-B magnet as a substrate

Peishu Song<sup>1</sup>, Zhenyuan Liu<sup>1</sup>, Yan Li<sup>2</sup>, Dan Han<sup>3</sup>, \*Lanting Zhang<sup>1</sup> (1. Shanghai Jiao Tong University (China), 2. Inner Mongolia University of Science and Technology (China), 3. Inner Mongolia Research Institute of Shanghai Jiao Tong University (China))

---

[P1-63]

### Microstructural Investigation of Nd-Fe-B Magnets Fabricated by Laser Powder Bed Fusion

\*Hojeong Kim<sup>1</sup>, Taesuk Jang<sup>2</sup>, Du-Rim Eo<sup>3</sup>, Wooyoung Lee<sup>1</sup> (1. Yonsei university (Korea), 2. Sunmoon University (Korea), 3. KITECH (Korea))

---

[P1-64]

### From Scrap to Bonded Magnet: Exploring Nanocrystalline Recycled Powders in Additive Manufacturing

\*Marcelo Augusto Rosa<sup>1</sup>, Gabriel Maia<sup>2</sup>, Apuniano Baldarrago<sup>1</sup>, Maximiliano Martins<sup>2</sup>, Paulo Wendhausen<sup>1</sup> (1. UFSC (Brazil), 2. CDTN (Brazil))

---

[P1-65]

### Enhancing the Printability of Nd-Fe-B Feedstocks for Laser Powder Bed Fusion

Marcelo Augusto Rosa<sup>1</sup>, Apuniano Baldarrago<sup>1</sup>, Arthur Mascheroni<sup>2</sup>, José Maria Mascheroni<sup>2</sup>, \*Paulo Wendhausen<sup>1</sup> (1. UFSC (Brazil), 2. Alkimat (Brazil))

[P1-66]

Preparation of micromagnets via LIFT technique

\*Masaki Nakano<sup>1</sup>, Gakuto Tahara<sup>1</sup>, Takuki Amiya<sup>1</sup>, Akihiro Yamashita<sup>1</sup>, Takeshi Yanai<sup>1</sup>, Masaru Itakura<sup>2</sup>, Kunihiro Koike<sup>3</sup>, Hirotoshi Fukunaga<sup>1</sup> (1. Nagasaki university (Japan), 2. Kyushu university (Japan), 3. Yamagata university (Japan))

[P1-67]

Sputtered high-coercivity CeCo thin film on glass substrate

Cheng-Yan Lee<sup>2</sup>, Sea-Fue Wang<sup>2</sup>, Huang-Wei Chang<sup>3</sup>, \*An-Cheng Aidan Sun<sup>1</sup> (1. Yuan Ze University (Taiwan), 2. National Taipei University of Technology (Taiwan), 3. National Chung Cheng University (Taiwan))

[P1-68]

Growth of SmFe<sub>12</sub> thin films using MBE

\*Uyanga Enkhnanan<sup>1</sup>, Jargalan Narmandakh<sup>1</sup>, Sangaa Deleg<sup>1</sup>, Uranbaigal Enkhtur<sup>2</sup>, Odkhuu Dorj<sup>2</sup>, Sunglae Cho<sup>3</sup> (1. Institute of Physics and Technology of Mongolian Academy of Sciences (Mongolia), 2. Incheon National University (Korea), 3. University of Ulsan (Korea))

[P1-69]

Development of data handling tools for high-throughput experiments

\*Pierre Le Berre<sup>1</sup>, William Rigaut<sup>1</sup>, Wilfried Hortschitz<sup>2</sup>, Santa Pile<sup>2</sup>, Harald Oezelt<sup>2</sup>, Samuel J. R. Holt<sup>3,4</sup>, Swapneel A. Pathak<sup>3,4</sup>, Hans Fangohr<sup>3,4,5</sup>, Thomas Schrefl<sup>2</sup>, Thibaut Devillers<sup>1</sup>, Nora M. Dempsey<sup>1</sup> (1. Univ. Grenoble Alpes, CNRS, Grenoble INP, Institut Néel, 38000 Grenoble (France), 2. Department for Integrated Sensor Systems, University for Continuing Education Krems, Wr. Neustadt (Austria), 3. Max Planck Institute for the Structure and Dynamics of Matter, Luruper Chaussee 149, 22761 Hamburg (Germany), 4. Center for Free-Electron Laser Science, Luruper Chaussee 149, 22761 Hamburg (Germany), 5. Faculty of Engineering and Physical Sciences, University of Southampton, Southampton SO17 1BJ (UK))

[P1-70]

Towards the high-throughput microstructural characterisation of compositionally graded NdFeB-based films

\*Lukas Fink<sup>1</sup>, William Rigaut<sup>1</sup>, Pierre Le-Berre<sup>1</sup>, Heisam Moustafa<sup>2</sup>, Qais Ali<sup>2</sup>, Leoni Breth<sup>2</sup>, Thomas Schrefl<sup>2</sup>, Harald Oezelt<sup>2</sup>, Thibaut Devillers<sup>1</sup>, Nora M. Dempsey<sup>1</sup> (1. 1Université Grenoble Alpes, CNRS, Grenoble INP, Institut Néel, 38000 Grenoble (France), 2. Department for Integrated Sensor Systems, University for Continuing Education Krems, 2700 Wr. Neustadt (Austria))

[P1-71]

Characterization of rare earth garnet [Eu<sub>3</sub>Fe<sub>5</sub>O<sub>12</sub>/Tb<sub>3</sub>Fe<sub>5</sub>O<sub>12</sub>]/Gd<sub>3</sub>Ga<sub>5</sub>O<sub>12</sub> (111) ([EuIG/TbIG]/GGG (111)) thin films

\*Ko-Wei Lin<sup>1</sup>, Guan-Hua Lu<sup>1</sup>, Tai-Yi Chiu<sup>1</sup>, Chi Wah Leung<sup>2</sup> (1. National Chung Hsing University (Taiwan), 2. The Hong Kong Polytechnic University (China))

[P1-73]

Effect of Ir addition on the crystal structure and magnetic properties for Mn-Ga thin films

\*Yuto Yamazaki<sup>1</sup>, Masaaki Doi<sup>1</sup>, Toshiyuki Shima<sup>1</sup> (1. Tohoku Gakuin University (Japan))

[P1-74]

## Magnetocaloric effect of textured polycrystalline $RNi_5$ alloys

\*Iurii Koshkidko<sup>1</sup>, Jacek Ćwik<sup>1</sup> (1. Institute of Low Temperature and Structure Research, PAS, Okólna 2, Wrocław, 50-422 (Poland))

---

[P1-75]

The influence of phosphorization treatment on the high-temperature oxidation resistance of Nd-Fe-B magnetic powder

\* Jingwu Zheng<sup>1</sup>, Xinqi Zhang<sup>1</sup>, Dongsheng Shi<sup>1</sup>, Wei Cai<sup>1</sup>, Liang Qiao<sup>1</sup>, Yao Ying<sup>1</sup>, Shenglei Che<sup>1</sup> (1. Research Center of Magnetic and Electronic Materials, College of Materials Science and Engineering, Zhejiang University of Technology, Hangzhou 310014, China (China))

---

📅 Mon. Jul 28, 2025 4:30 PM - 6:00 PM JST | Mon. Jul 28, 2025 7:30 AM - 9:00 AM UTC 🏠 Yellow zone, Conference rooms 101 and 102(1F)

## [P1] Processing, Characterization & Thin Films

Session Chair: Dr. Imants Dirba (Technical University of Darmstadt, Germany), Dr. Tae-Hoon Kim (Korea Institute of Materials Science, Korea)

### [P1-50] Optimization of Processing Parameters for High-Performance Anisotropic Bonded Magnets

\*Ikenna C. Nlebedim<sup>1</sup>, Xubo Liu<sup>1</sup>, Parans Paranthaman<sup>2</sup> (1. Division of Critical Materials, Ames National Laboratory (United States of America), 2. Chemical Sciences Division, Oak Ridge National Laboratory (United States of America))

Keywords : Anisotropic bonded magnets、Magnetic alignment、Rare earth elements magnets、Near-net-shape fabrication、Permanent magnet optimization

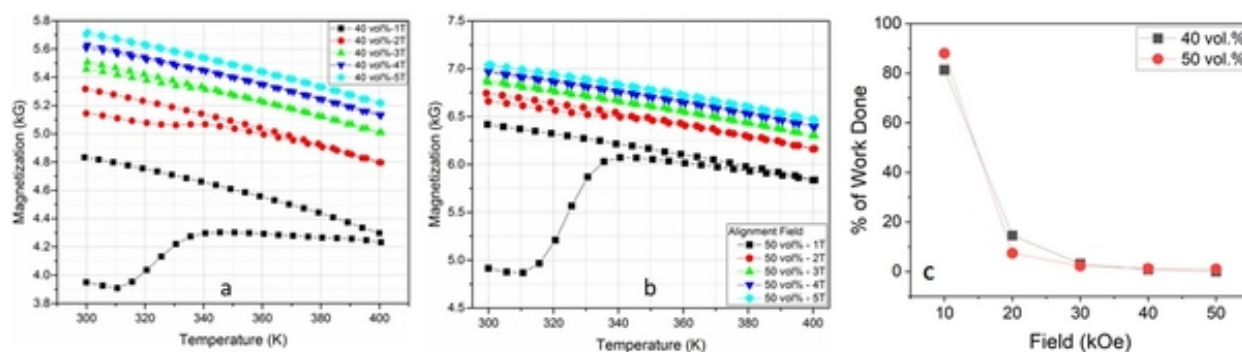
This study relates to the correlation between key physical parameters governing the processing of anisotropic bonded magnets. These parameters include the magnetic loading fraction, binder rheological properties, externally applied magnetic field strength, the interaction between the magnet particles, and the degree of particle alignment. Understanding, optimizing and controlling these interdependent variables are crucial for the fabrication of high-performance bonded magnets while concurrently minimizing rare earth (REE) content.

The use of sintered Nd-Fe-B magnets in compact electronic applications frequently necessitates extensive machining which results in significant material wastage [1], [2]. In contrast, bonded magnets, which can be fabricated via near-net-shape processing, can significantly reduce machining-induced waste and, consequently, lead to REE materials resource efficiency. Additionally, given the intrinsically lower magnet fraction in bonded magnets compared to sintered magnets, there exists an opportunity for further reduction in critical REE utilization in applicable devices/systems. Thus, bonded magnets present a viable strategy for mitigating potential supply chain disruptions of REE materials essential for permanent magnet applications.

In this study, bonded magnets were synthesized through extrusion processing of anisotropic MQA powder at 40 and 50 vol.% loadings with an ethylene-vinyl acetate (EVA) copolymer binder. Differential scanning calorimetry (DSC) was employed to characterize the thermal transitions of EVA, both in pristine form and in composite formulations with magnetic powders. Magnetic hysteresis measurements and magnetization (M vs. T) as a function of temperature studies were conducted using a SQUID magnetometer, which also enabled the controlled alignment of samples during processing.

Figure 1 illustrates the M vs. T profiles for the 40 vol.% and 50 vol.% samples subjected to varying alignment field strengths. At an applied field of  $\mu_0 H = 1$  T, both compositions reached maximum alignment at approximately 340 K. The results demonstrate that alignment commences at the onset of EVA melting (~310 K) and culminates at ~340 K.

Comparing Fig. 1a and 1b, the change in magnetization between the heating and cooling steps is less for the 50 vol.% sample, relative to the 40 vol.% sample. This result suggests that the degree of alignment achieved, especially at  $\mu_0 H = 1$  T, is higher for the 50 vol.% sample, compared to the 40 vol.% sample. Fig. 1c shows that  $\mu_0 H = 1$  T accomplished more than 80 vol% of the work needed to align the particles. This behavior is due to competing interactions, i.e., Zeeman energy, magnetostatic energy, and the drift force between molten binder and particles. A comprehensive understanding of these competing forces is paramount for refining processing parameters and optimizing the functional performance of bonded magnets.



Poster | Material, processing, and characterization

📅 Mon. Jul 28, 2025 4:30 PM - 6:00 PM JST | Mon. Jul 28, 2025 7:30 AM - 9:00 AM UTC 🏠 Yellow zone, Conference rooms 101 and 102(1F)

## [P1] Processing, Characterization & Thin Films



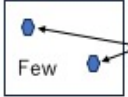
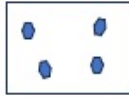


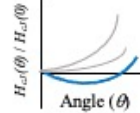
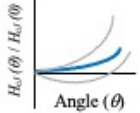
Session Chair: Dr. Imants Dirba (Technical University of Darmstadt, Germany), Dr. Tae-Hoon Kim (Korea Institute of Materials Science, Korea)

### [P1-51] Demagnetization Processes in Nd-Fe-B sintered and Ferrite Magnets derived from magnetic measurement and soft X-ray magnetic circular dichroism microscopy

\*Yutaka Matsuura<sup>1</sup> (1. Research Institute for Applied Sciences (Japan))

Keywords : Nd-Fe-B sintered magnet, ferrite magnet, demagnetization, coercivity, coercivity mechanism

Demagnetization processes of Nd-Fe-B sintered and ferrite magnets were investigated via magnetic measurements and soft X-ray magnetic circular dichroism microscopy (XMCD). From the alignment dependence, the coercivities of these magnets were determined by magnetic domain wall motion because it decreased with improved alignment. The alignment dependence of coercivity varies according to the compositions and manufacturing methods due to the cluster sizes of demagnetization grains at their coercivity. The sizes increased with decreasing temperature and varied with composition. The continuous small demagnetization was observed in the recoil curve in a demagnetization field smaller than their coercivity. From XMCD, the magnetization reversal of individual particles was observed in a small demagnetization field, and clusters of demagnetization grains were formed from reversals of neighboring particles at the discretely demagnetized particle near its coercivity. The cluster growth yielded coercivity, and it was speculated that cluster sizes were related to their alignments and angular dependences of their coercivities. They also depended on the number of discretely demagnetized particles that occurred in a smaller demagnetization field than their coercivity.

Temperature	Low  High				
Composition	$(\text{Pr}_{17}\text{Fe}_{75}\text{B}_8)$ ( $\text{Pr}_{17}\text{Fe}_{63}\text{B}_{30}$ ) at 4.2K	$\text{Nd}_{14.79}\text{Ga}_{0.57}\text{B}_{5.24}\text{Co}_{1.11}\text{Fe}_{\text{bal}}$ at R.T.	$\text{SrO} \cdot 6\text{Fe}_2\text{O}_3$ at R.T.	$\text{Nd}_{14.2}\text{Dy}_{9.2}\text{B}_{9.2}\text{Co}_{1.0}\text{Fe}_{\text{bal}}$ at R.T.	$\text{Nd}_{14.2}\text{B}_{9.2}\text{Co}_{1.0}\text{Fe}_{\text{bal}}$ at R.T.
Magnetization Reverse Area ( $\theta_{\text{ms}}$ )	( $\sim 45^\circ$ )	$41.7^\circ$	$40.6^\circ$	$36^\circ$	$30^\circ$
Cluster size of reversed grains at $H_{cJ}$	Large  Small				
Number of discretely reverse grains before cluster formation)					
Alignment dependence ( $\beta$ ) of $H_{cJ}$					
Angular dependence of $H_{cJ}$ ( $H_{cJ}(\theta) / H_{cJ}(0)$ )					



📅 Mon. Jul 28, 2025 4:30 PM - 6:00 PM JST | Mon. Jul 28, 2025 7:30 AM - 9:00 AM UTC 🏠 Yellow zone, Conference rooms 101 and 102(1F)

## [P1] Processing, Characterization & Thin Films

Session Chair: Dr. Imants Dirba (Technical University of Darmstadt, Germany), Dr. Tae-Hoon Kim (Korea Institute of Materials Science, Korea)

### [P1-52] Anisotropy field measurement in hard magnets: evaluating current methodologies

\*Alex Aubert<sup>1</sup>, Konstantin Skokov<sup>1</sup>, Oliver Gutfleisch<sup>1</sup> (1. Functional Materials, TU Darmstadt (Germany))

Keywords : Anisotropy field、 methodology

With the exponential rise of data-driven materials research strategies, datasets play a crucial role in developing models and predicting material properties. However, machine learning requires accurate datasets and well-defined descriptors to ensure reliable predictions [1]. In the field of energy applications, the demand for high-performance and sustainable permanent magnets is growing, and machine learning has the potential to accelerate the discovery of new compositions. One of the key criteria for achieving hard magnetic properties is the anisotropy field  $H_A$  [2].

Traditionally,  $H_A$  is determined by using single crystals of a defined shape. However, growing phase-pure single crystals is not always feasible for certain hard magnetic compounds due to phase stability challenges. Researchers therefore employ alternatives such as aligned polycrystalline powder, but the results are not always accurate. In this study, we compare and evaluate the most commonly used methodologies for estimating the anisotropy field using  $\text{Ce}_2\text{Fe}_{14}\text{B}$  as a case study. Specifically, we assess different methods—including hard-axis saturation, magnetization area, Sucksmith-Thompson (S-T), the law of approach to saturation (LAS), and singular point detection (SPD)—applied to single crystals, aligned polycrystals powder, and isotropic bulk polycrystals.

Our results show that for single crystals, most of the methods provide accurate results within a 2% relative error when the demagnetizing field is properly accounted for. However, without demagnetizing field correction, an error of 9.5% was obtained in our case. The highest errors in  $H_A$  are observed for aligned polycrystalline powders, reaching up to 17% compared to single-crystal data. Notably, the SPD method based on the first derivative of the magnetization curve, widely used in recent literature, did not provide accurate results for single crystals or aligned polycrystals. The underlying reasons are discussed in detail. In contrast, the SPD method utilizing a pulse magnetometer with second derivative analysis provides a reliable estimation of the anisotropy field for both single crystals and polycrystals (see Figure). These findings are particularly relevant for materials scientists seeking to use reliable descriptors in machine learning datasets and to accurately estimate the anisotropy field in new hard magnetic compounds.

## References:

- [1] R. Ramprasad *et al.* *npj Comput Mater* **3**, 54 (2017)  
 [2] R. Skomski, and J. M. D. Coey. *Scripta Materialia* 112 (2016): 3-8.

## Acknowledgement:

This work was supported by the Deutsche Forschungsgemeinschaft (DFG, German Research Foundation), Project ID no. 405553726-TRR 270.

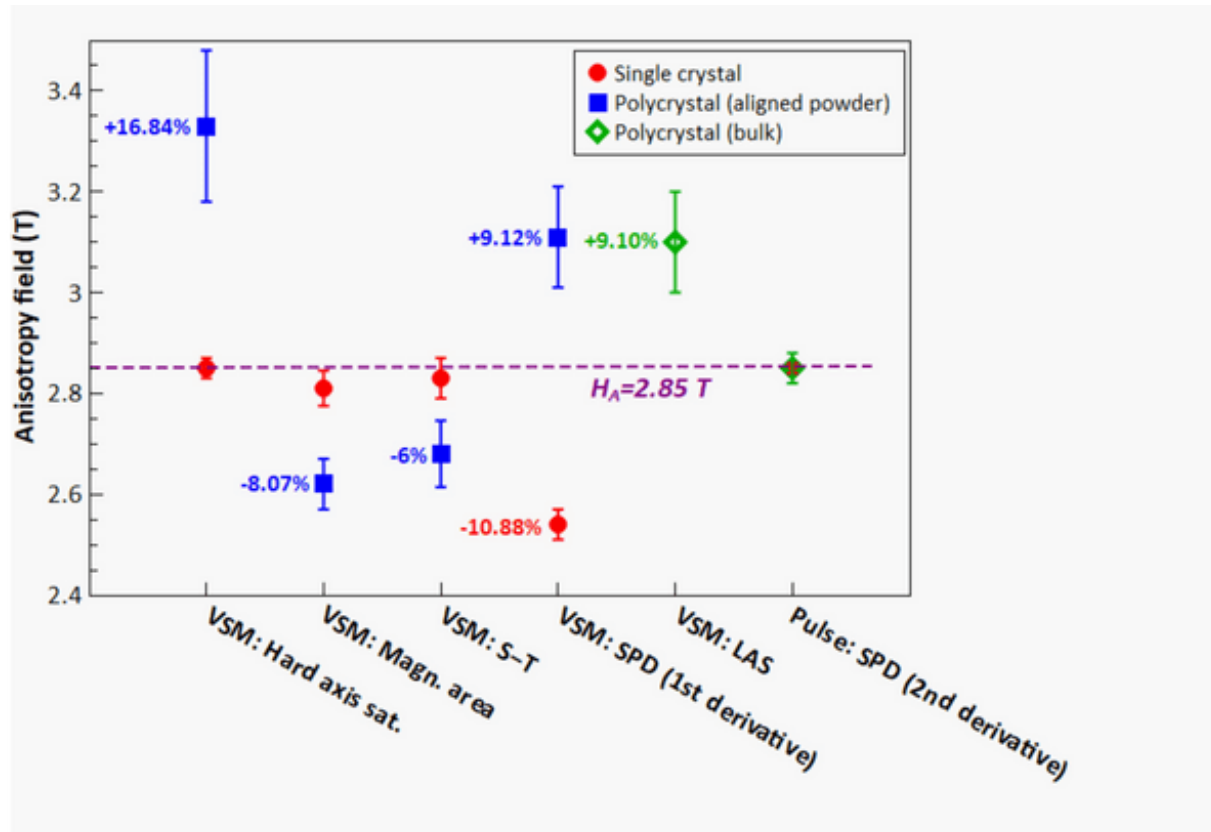


Figure: Comparison of anisotropy field obtained for various methods and types of samples (single crystal, aligned polycrystal and bulk polycrystal). The relative error in percentage is added next to the points when superior to 5%.

📅 Mon. Jul 28, 2025 4:30 PM - 6:00 PM JST | Mon. Jul 28, 2025 7:30 AM - 9:00 AM UTC 🏠 Yellow zone, Conference rooms 101 and 102(1F)

## [P1] Processing, Characterization & Thin Films

Session Chair: Dr. Imants Dirba (Technical University of Darmstadt, Germany), Dr. Tae-Hoon Kim (Korea Institute of Materials Science, Korea)

### [P1-53] Angular Dependence of Coercivity and Flux Loss under Tilted Field in Nd-Fe-B Sintered Magnet

\*Hitoshi Yamamoto<sup>1</sup>, Hirotohi Fukunaga<sup>2</sup> (1. Neoji-consul (Japan), 2. Nagasaki University (Japan))

Keywords : Nd-Fe-B magnet、 coercive force、 differential coercive force、 demagnetization、 angular dependence

In order to implement effectively Nd-Fe-B magnets for many applications such as industrial, automotive and home appliance uses, it is important to evaluate the demagnetization properties of magnets against demagnetization field  $H_d$ . In case of FA/OA and EV/HV motor applications, magnets may be often exposed under  $H_d$ , not only the direction of magnetic polarization  $J$  but also the tilted direction from  $J$ . However little papers have been reported on the demagnetization properties under the tilted demagnetization field.

The authors executed the demagnetization experiments with varying the directions and magnitude of the pulsed demagnetization field  $H_d$ , evaluating the flux loss  $FL$  on the surface of the magnet, and compared the results of  $FL$  with the measured data of the angular dependence of coercivity.

The tested Nd-Fe-B magnet is a commercially available grade N46H, of which measured magnetic properties;  $B_r=1.34\text{T}$ ,  $H_{cJ}=1,506\text{ kA/m}$ . The result of flux loss  $FL$  is plotted in Fig. 1 as a function of the magnitude of  $H_d$  for  $\theta=0, 45, 70$  and  $90$  degree, where  $\theta$  is the angle between the direction of magnetic polarization  $J$  and the applied pulsed field  $H_d$ . In case of  $\theta=0$  and  $45$  degree, the flux was constant up to the demagnetization field  $H_d$  of  $500\text{ kA/m}$ , and gradually decreased with increasing  $H_d$ , and finally fully demagnetized at  $1,500\text{ kA/m}$ , which is the same value of the coercive force of the magnet. The demagnetization features of  $\theta=0$  and  $45$  degree are exactly same, while the field to start to occur the demagnetization for  $\theta=70$  and  $90$  degree is  $800$  and  $1,300\text{ kA/m}$  respectively, which values are much higher than the values of  $500\text{ kA/m}$  for  $\theta=0$  and  $45$  degree.

To consider the flux loss  $FL$  results of Fig.1, the angular dependences of coercive force  $H_{cJ}$  and  $H_{cJD}$  was measured and shown in the inset in Fig.1, where  $H_{cJD}$  is the derivative coercive force, which is tentatively defined as the magnetic field corresponding to the maximum of  $dJ/dH$ . As clearly seen in the inset in Fig.1, the values of  $H_{cJ}$  and  $H_{cJD}$  are same at  $\theta=0$  and  $45$  degree. Both values are same up to the angle of  $60$  degree, but over  $70$  degree the value of  $H_{cJ}$  decreases rapidly, while  $H_{cJD}$  increases gradually with increasing the tilted angle  $\theta$ . The increase of  $H_{cJD}$  for  $\theta=70$  and  $90$  degree is consistent with the

results of flux loss  $FL$  for  $\theta = 70$  and  $90$  degree in Fig.1.

It is strange that the demagnetization properties for the tilted angle  $\theta = 0$  and  $45$  degree is the same feature, because the demagnetization field with  $J$  direction component for  $\theta = 45$  degree is much weaker than  $\theta = 0$  degree, theoretically  $1/\sqrt{2}$ . Reviewing both results of Fig.1 and the inset, the demagnetization feature of Fig.1 is related with the angular dependence of the value of  $H_{cJD}$  not the value of  $H_{cJ}$ . The  $H_{cJD}$  is determined by the irreversible rotation, while  $H_{cJ}$  reflects both irreversible and reversible rotation of the magnetic polarization  $J$ . Demagnetization of magnets is the phenomena of irreversible magnetic reversal process, therefore it is reasonable to consider that  $H_{cJD}$  is the appropriate parameter to evaluate demagnetization properties of magnets.

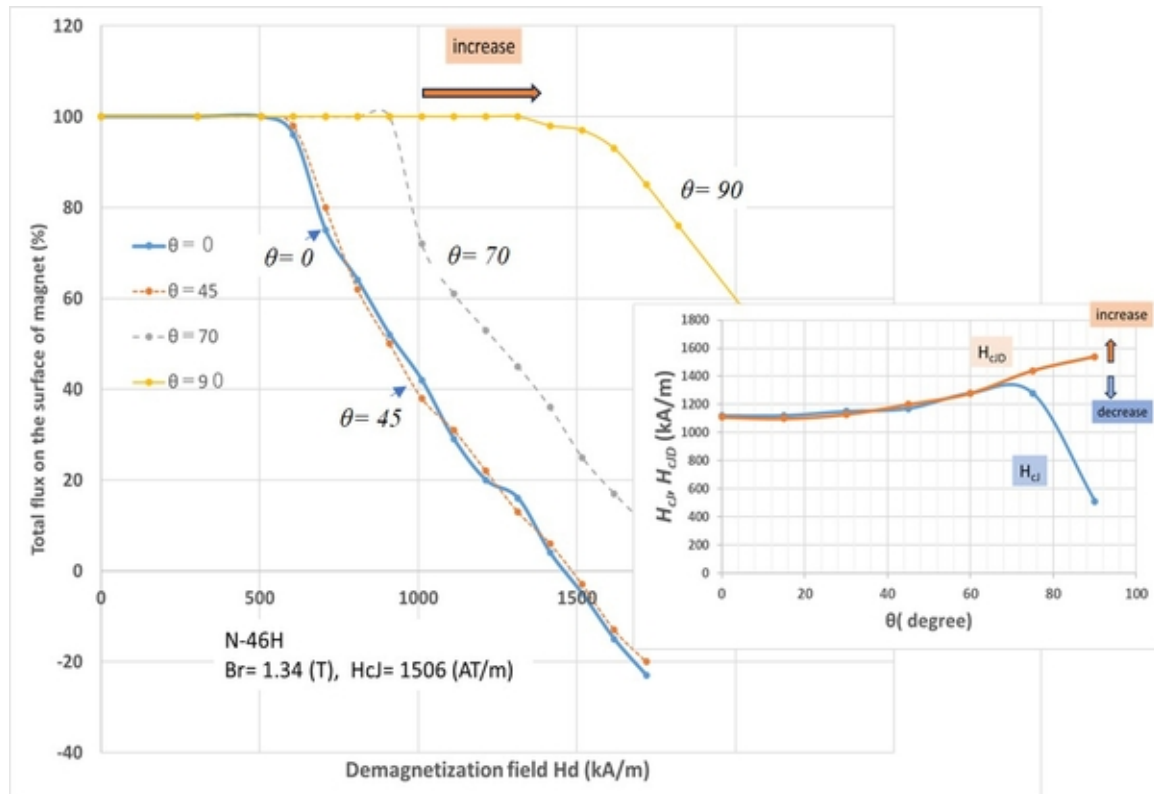


Fig.1 ; Flux on the surface of the magnet vs demagnetization field  $H_d$  for  $\theta = 0, 45, 70$  and  $90$  degrees

The inset;  $H_{cJ}$  and  $H_{cJD}$  vs tilted angle  $\theta$

Poster | Material, processing, and characterization

📅 Mon. Jul 28, 2025 4:30 PM - 6:00 PM JST | Mon. Jul 28, 2025 7:30 AM - 9:00 AM UTC 🏛️ Yellow zone, Conference rooms 101 and 102(1F)

## **[P1] Processing, Characterization & Thin Films**

Session Chair: Dr. Imants Dirba (Technical University of Darmstadt, Germany), Dr. Tae-Hoon Kim (Korea Institute of Materials Science, Korea)

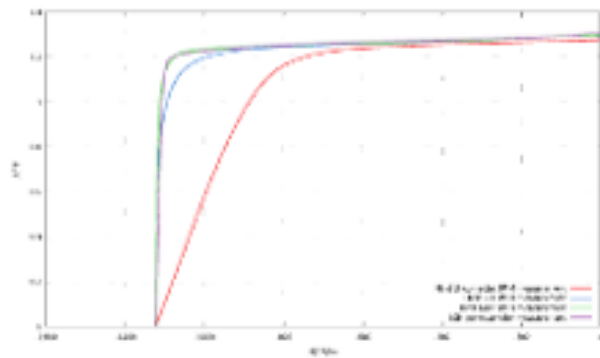
[P1-54] Pulsed Field Magnetometers - validating data generated by Self-Demagnetisation Field Function (SDFF) correction to create closed loop results from open loop measurements

\*Robin Cornelius<sup>1</sup>, Jian He<sup>2</sup>, Jack Wade<sup>1</sup>, Stuart Harwin<sup>1</sup>, James Mckenzie<sup>1</sup> (1. Hirst Magnetic Instruments Ltd (UK), 2. National Institute of Metrology (China))

Keywords : BH loops、 Pulsed Field Magnetometer、 Rare Earth Permanent Magnet Characterisation

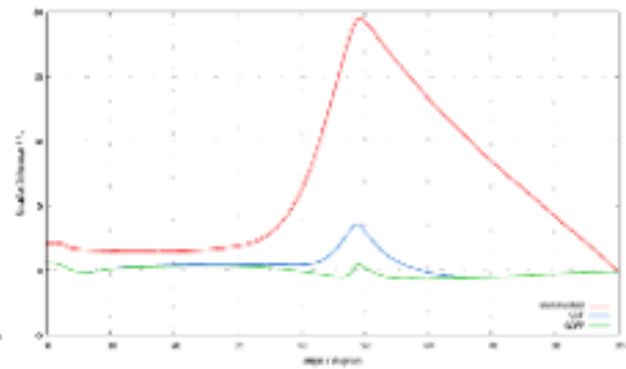
The Hirst PFM08 range of magnet characterisation magnetometer launched in 2023 can rapidly and accurately measure the magnetic hysteresis loop and extract key values for all high-grade permanent magnetic materials such as NdFeB, SmCo, Ferrite and all coated magnets. With a maximum field of 10.5T (8356 kA/m / 105 kOe) even the most coercive materials and highest grades of NdFeB or SmCo can be measured, while traditional permeameters cannot measure these high coercivity materials due to pole piece saturation limitations. The 8th generation of PFMs from Hirst feature the eddy current correction (patented F-2F algorithm), Self-Demagnetisation Field (SDF) correction function (to allow accurate measurement of a wide range of samples from cylinders, cuboids and arbitrary sample shapes), and Hirst proprietary Self De-magnetisation Field Function SDFF<sup>TM</sup> (patented) which accurately generates an open to closed circuit mapping. SDFF technology has been implemented in collaboration with the National Institute of Metrology (NIM), Beijing, as part of a contract for the first 8th generation PFM placed by NIM in 2023. This paper will present the detailed results that validate the SDFF algorithm validating the claim that the results are within 1% of NIM permeameter reference measurements on standard reference samples

## SDFF results Summary



Across the demagnetisation quadrant:

- Typical peak error is <1%
- Typical integrated error <1%



Above we show the difference function between data from a permeameter measurement and:

- Uncorrected PFM measurement
- SDF PFM measurement
- SDFF PFM measurement

Poster | Material, processing, and characterization

📅 Mon. Jul 28, 2025 4:30 PM - 6:00 PM JST | Mon. Jul 28, 2025 7:30 AM - 9:00 AM UTC 🏢 Yellow zone, Conference rooms 101 and 102(1F)

## [P1] Processing, Characterization & Thin Films

Session Chair: Dr. Imants Dirba (Technical University of Darmstadt, Germany), Dr. Tae-Hoon Kim (Korea Institute of Materials Science, Korea)

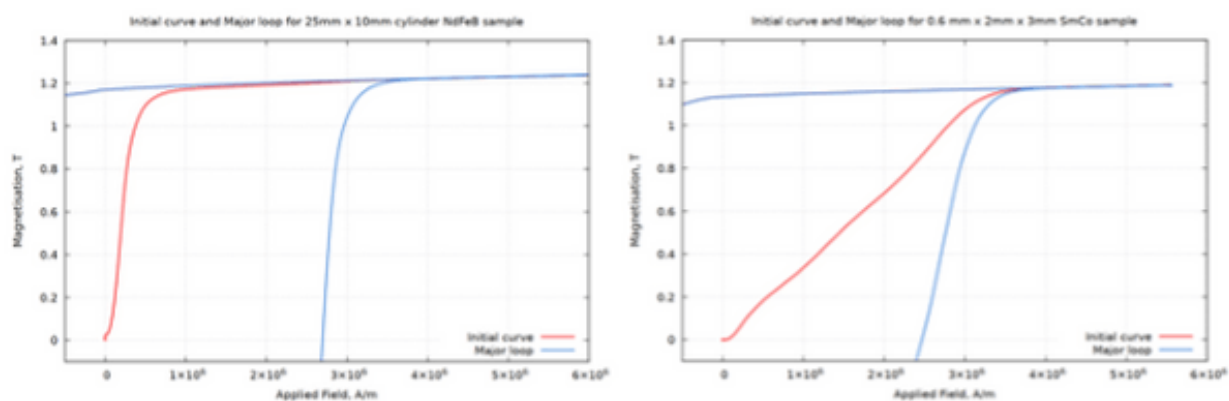
### [P1-55] Measuring initial curves and minor hysteresis loops for rare earth magnets using the Pulsed Field Magnetometer (PFM) system

\*Robin Cornelius<sup>1</sup>, Jack Wade<sup>1</sup>, Stuart Harwin<sup>1</sup>, James Mckenzie<sup>1</sup> (1. Hirst Magnetic Instruments Ltd (UK))

Keywords : Pulsed Field Magnetometer、BH Loop - initial curves and minor loops、SmCo、NdFeB、FORC diagrams

This presentation will review recent progress and results gained from the Hirst generation 8 Pulsed Field Magnetometers on initial magnetisation curves, minor loops being applied to samples and the implementation of First Order Reversal Curves (FORCs) on a PFM. The initial curve represents the initial magnetization process of a permanent magnet from when it is completely unmagnetized. This curve is important for understanding the composition, metallurgy, and microstructure of a material. We will present results for NdFeB and SmCo magnets. Minor Loops are generated when the applied magnetic field is reversed but does not reach the saturation point, creating smaller loops within the main hysteresis loop. This provides information about the reversibility of magnetization within a specific field range and can be used to analyse the stability of a permanent magnet under changing magnetic fields. We will present results for NdFeB magnets. First order reversal curve (FORC) measurements provide insight into the magnetic properties of materials, information that is not possible to obtain from a full hysteresis loop alone or individual minor loops. FORC curves help in identifying the distribution of switching and interaction fields, and in distinguishing between multiple magnetic phases in composite or hybrid materials containing more than one phase of magnetic materials. This information can be used to analyse magnet production techniques and novel materials. We will present results for NdFeB magnets. This new option on the latest generation 8 PFMs from Hirst and takes advantage of the full pulsed field that drives the sample through all four quadrants of the hysteresis loop during a measurement.

## Initial curve measurements on PFM



Measurements of two different samples showing the initial curve (red) and the major loop (blue) for that sample. These measurements were taken using an 8<sup>th</sup> generation Hirst Pulsed Field Magnetometer (PFM). On the left is a relatively large 25mm (height) x 10mm (diameter) cylinder of NdFeB. On the right is a small 0.6mm (height) x 2mm x 3mm SmCo sample.



📅 Mon. Jul 28, 2025 4:30 PM - 6:00 PM JST | Mon. Jul 28, 2025 7:30 AM - 9:00 AM UTC 🏠 Yellow zone, Conference rooms 101 and 102(1F)

## [P1] Processing, Characterization & Thin Films

Session Chair: Dr. Imants Dirba (Technical University of Darmstadt, Germany), Dr. Tae-Hoon Kim (Korea Institute of Materials Science, Korea)

### [P1-56] Spectroscopic insights into the electronic structure of non-critical rare earth containing permanent magnets

\*Benedikt Eggert<sup>1</sup>, Alex Aubert<sup>2</sup>, Philipp Klaben<sup>1</sup>, Janosch Tasto<sup>1</sup>, Nathan Yutronkie<sup>3</sup>, Fabrice Wilhelm<sup>3</sup>, Andrei Rogalev<sup>3</sup>, Konstantin Skokov<sup>2</sup>, Heiko Wende<sup>1</sup>, Oliver Gutfleisch<sup>2</sup>, Katharina Ollefs<sup>1</sup> (1. University of Duisburg-Essen (Germany), 2. Technical University of Darmstadt (Germany), 3. European Synchrotron Radiation Facility (France))

Keywords : X-ray absorption spectroscopy, Ce based compounds, X-ray magnetic circular dichroism

The extensive use of critical rare-earth elements like Nd and Sm in magnet production raises concerns about their limited availability. Ongoing research explores the feasibility of cost-effective hard magnetic materials by substituting Nd or Sm with more abundant rare-earth elements such as Ce or La [2]. Here, it is crucial to deepen the understanding of compounds' electronic and magnetic structures consisting of these low-cost rare-earth elements. Within this contribution, we focus on investigating the magnetic properties and electronic structures of Ce-containing permanent magnets in compounds such as  $(\text{Nd,Ce})_2\text{Fe}_{14}\text{B}$  [3],  $\text{CeCo}_5$  [4], or  $\text{CeFe}_{11}\text{Ti}$  [5]. Therefore, we employ advanced spectroscopic techniques, for example, X-ray absorption spectroscopy or X-ray magnetic circular dichroism, by probing the rare earth L<sub>2,3</sub> and transition metal K edges. With this spectroscopic approach, we gain element-specific insights into the electronic structure and resolve the magnetic properties of each element in these systems. In particular, we will show how Ce's valence state can be manipulated, e.g., by modifying its local surroundings. Here, we will show that adding Cu in  $\text{CeCo}_5$  compounds leads to the formation of a Cu-rich region, resulting in a paramagnetic  $\text{Ce}^{3+}$  state that can act as a pinning site of domain walls. In the  $\text{CeFe}_{11}\text{Ti}$  system, introducing interstitial N leads to an enhanced Kondo screening of the 4f electrons [5], resulting in a reduction of the magnetic anisotropy.

We acknowledge the financial support through the Deutsche Forschungsgemeinschaft within the framework of the CRC/TRR270 HoMMage (Project 405553726-TRR270), the BMBF (05K2019 and 05K2022), and we thank the ESRF for allocation of beamtime at beamline ID12 within projects HC-4051 & MA-5882.

#### References

- [1] O. Gutfleisch et al. Adv. Mater. 23, 821-842 (2011)
- [2] K. P. Skokov et al. Scripta Materialia, 154, 289-294 (2018)
- [3] Y. Wu et al. Acta Materialia, 235, 118062 (2022)

- [4] H. Shishido J. Magn. Magn. Mater. 562, 169748 (2022)
- [5] A. Galler et al. npj Quantum Materials 6, 2 (2021)

📅 Mon. Jul 28, 2025 4:30 PM - 6:00 PM JST | Mon. Jul 28, 2025 7:30 AM - 9:00 AM UTC 🏠 Yellow zone, Conference rooms 101 and 102(1F)

## [P1] Processing, Characterization & Thin Films

Session Chair: Dr. Imants Dirba (Technical University of Darmstadt, Germany), Dr. Tae-Hoon Kim (Korea Institute of Materials Science, Korea)

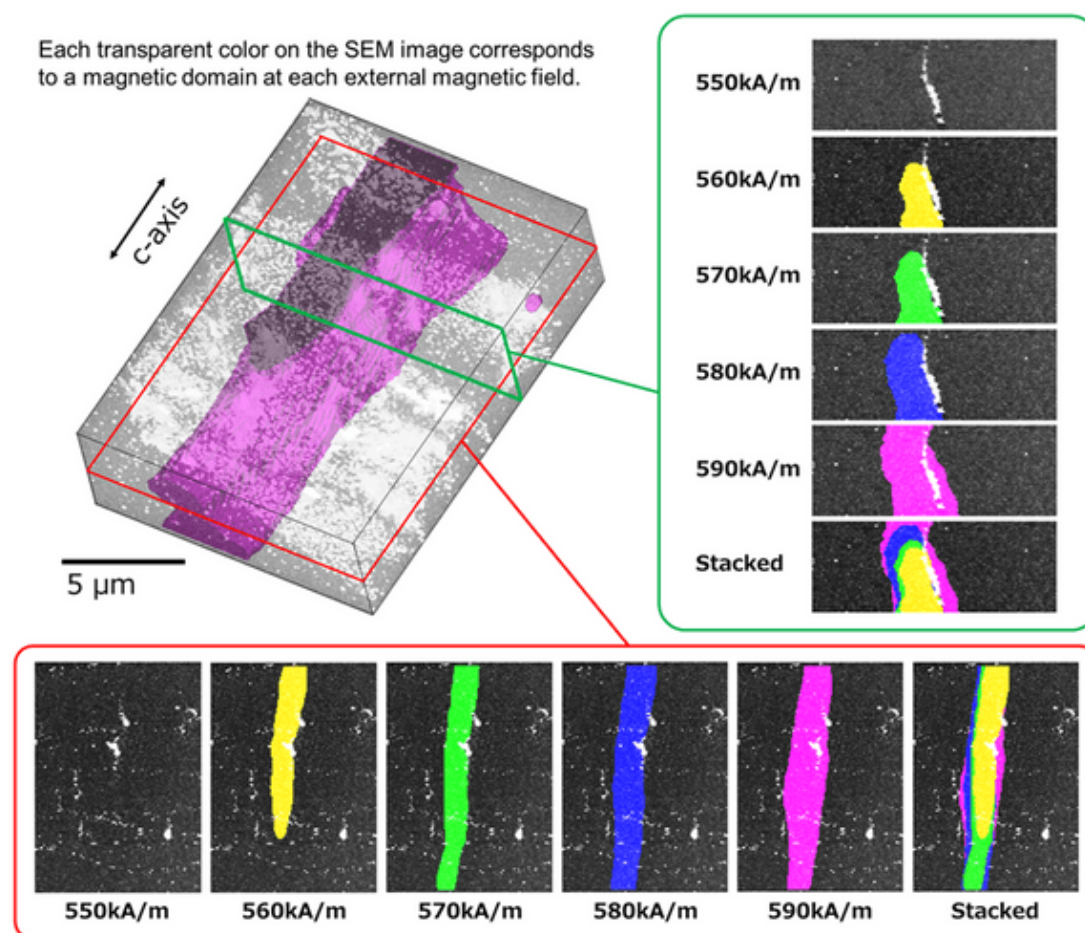
### [P1-57] Three-dimensional magnetic domain propagation of a Nd-Fe-B hot-deformed magnet

\*Tomomi Suwa<sup>1</sup>, Motohiro Suzuki<sup>2</sup>, Tadakatsu Ohkubo<sup>3</sup>, Iriyama Takahiko<sup>4</sup>, Hiroshi Miyawaki<sup>4</sup>, Kaiki Takemura<sup>2</sup>, Yusuke Akiyama<sup>2</sup>, Takuya Taniguchi<sup>1</sup>, Satoshi Okamoto<sup>1,3</sup> (1. Tohoku University (Japan), 2. Kwansei Gakuin University (Japan), 3. National Institute for Materials Science (Japan), 4. Daido Steel Company, Limited (Japan))

Keywords : Three-dimensional analysis、Magnetic reversal process、Magnetic domain、Microstructure、Nd-Fe-B magnet、Hot-deformed Nd-Fe-B magnet

The magnetization reversal mechanism of permanent magnets, particularly Nd-Fe-B magnets, involves interactions across multiple scales, including atomic spins, crystal lattices, grains, grain boundaries, and microstructures. This hierarchical complexity, coupled with the intricate nature of microstructures, has posed significant challenges in fully understanding the magnetization reversal process. A magnetization nucleation process has been elucidated gradually through the recent stochastic atomistic calculations of Nd<sub>2</sub>Fe<sub>14</sub>B grain<sup>1,2,3</sup>). However, the magnetization reversal in a bulk magnet takes place as nucleation of a reversed domain followed by domain propagation, and these processes have a strong relationship with the microstructure. To understand the magnetization reversal mechanism in bulk magnets, it is essential to observe the correlation between the microstructure and the magnetic domain evolution. Conventionally, two-dimensional(2D) observations of magnetic domain structure have been widely used, such as magnetic Kerr microscopy or a combination of scanning electron microscopy (SEM) and X-ray magnetic circular dichroism (XMCD) microscopy<sup>4,5</sup>). However, since the magnetic domain structure is inherently three-dimensional (3D), and unavoidable surface processing damage and demagnetizing fields make magnetic structures distorted, 2D observations are insufficient. Recently, our group developed a method combining 3D SEM and hard X-ray magnetic tomography, enabling 3D observation of microstructure and magnetic domain structure with the same spatial region<sup>6</sup>). In this study, we report the magnetization reversal process inside a hot-deformed Nd-Fe-B bulk magnet. The sample was a hot-deformed Nd<sub>30.9</sub>Fe<sub>bal.</sub>Co<sub>3.5</sub>B<sub>0.92</sub>Ga<sub>0.55</sub> magnet. It was mechanically polished and then processed into a shape of 18 μm × 18 μm (c-axis) × 45 μm using a focused ion beam (FIB). The 3D magnetic domain structure and X-ray absorption spectra (XAS) were acquired at the Nd L<sub>2</sub> edge using X-ray magnetic tomography with an algebraic reconstruction technique at BL39XU of SPring-8. Following this, the secondary and backscattered electrons images as 3D microstructure were obtained through FIB-SEM imaging. Alignment between the microstructure and magnetic domain structure was achieved using each Nd distribution obtained from backscattered electron images and XAS data.

The magnetic domain structure was measured focusing on the thermally demagnetized state and the state around the nucleation region of the hysteresis curve respectively. The minimum magnetic field interval was 10 kA/m, enabling the capture of gradual evolution in magnetic domains. However, due to the technical limits of the reconstruction algorithm, the magnetic domain images contained artifacts such as X-shaped and streak-shaped noises, which hindered precise analysis of magnetic domain evolution. To address this issue, flat-field correction, total variation regularization based on sparse modeling, and phase field calculation were applied for denoising. This combination of processing techniques effectively reduced noise, enabling the high-accuracy identification of magnetic domain positions and their evolution, as well as a precise analysis of magnetic domain wall dynamics inside the magnet. The figure shows the microscopic evolution of magnetic domains in the hot-deformed magnet, measured at intervals of 10 kA/m from 550 kA/m to 590 kA/m. At 550 kA/m, no magnetic domains were observed within the measurement area. As the magnetic field increased, magnetic domains propagated with slight changes. One of the key findings is that magnetic domains are strongly pinned in the large Nd-rich phase at the ribbon boundary. The Nd-rich phase at ribbon boundaries has been conventionally regarded as a nucleation site for magnetization reversal. However, our findings reveal that the large Nd-rich phase instead acts as a pinning site, inhibiting the propagation of the magnetic domain wall along the c-plane direction. [1]Y. Toga, et al., npj Computational Materials, 6, 67 (2020) [2]S. Miyashita, et al., STAM, 22,1(2021) [3]I. E. Uysal, et al., Phys. Rev. B, 101, 1, 094421(2020) [4] M. Takeuchi, et al., J. Japan Inst. Metals, 86, 1-7 (2022) [5] M. Takeuchi, et al., NPG Asia Materials, **14**, 70 (2022)



📅 Mon. Jul 28, 2025 4:30 PM - 6:00 PM JST | Mon. Jul 28, 2025 7:30 AM - 9:00 AM UTC 🏠 Yellow zone, Conference rooms 101 and 102(1F)

## [P1] Processing, Characterization & Thin Films

Session Chair: Dr. Imants Dirba (Technical University of Darmstadt, Germany), Dr. Tae-Hoon Kim (Korea Institute of Materials Science, Korea)

### [P1-58] A New Perspective on Assessing the Magnetic Texture in Nd-Fe-B Magnets: The influence of coercivity

Luis Torres Quispe<sup>1</sup>, \*Wagner Costa Macedo<sup>1</sup>, Marcelo Augusto Rosa<sup>1</sup>, Leonardo Antunes<sup>1</sup>, Apuniano Baldárrago-Alcántara<sup>1</sup>, Paulo Wendhausen<sup>1</sup> (1. Federal University of Santa Catarina (Brazil))

Keywords : Nd-Fe-B magnets、Texture determination、Magnetometry technique、Coercivity effect

Techniques like X-ray diffraction and electron diffraction are commonly used to determine texture of rare earth magnets. However, these techniques have some disadvantages, such as requiring time-consuming experiments, complex data analysis, a limited analysis volume compared to the size of an industrial magnet and higher infrastructure costs. The magnetometry technique is often used to determine the texture of NdFeB magnets and can offer significant advantages over diffractometry-based techniques. Fernengel et al 1996 were the first to propose this magnetometry technique for determining the texture of NdFeB magnets. However, the method was only applicable to highly textured magnets. Later, Quispe et al 2020 presented an improved version of Fernengel's method, which is applicable for any degree of texture. Although this magnetometry technique is reliable in determining texture values in most rare earth magnets, it can introduce error when applied to magnets with coercivity values above 900 kAm. In this study, we propose a method that provides a coercivity-dependent correction, allowing the magnetometry technique to remain a valid tool for magnets with any coercivity value. The methodology proposed here consists of determining the degree of alignment  $\cos\Theta$  from the values of the remanent magnetizations in the direction parallel  $J_r$  and perpendicular  $J_{r\perp}$  to the magnets texture axis, for which it is necessary to work with a parallelepiped or cubic-shaped magnet. The value of  $J_r$  is the easiest to obtain because the field applied by commercial pulse magnetizers are intense enough. On the other hand, obtaining  $J_{r\perp}$  is more complicated, as fields greater than the anisotropy field would be required. Applying a magnetic field pulse in the xy plane can induce some permanent magnetization due to the contribution of misaligned grains randomly distributed throughout the magnet. Different ways to calculate the field induced by this pulse are analyzed. The mathematical expression used to calculate  $J_{r\perp}$  in this newly proposed approach depends on the ratio  $F = H_c / H_{pulsed}$  where  $H_c$  is the average critical field for irreversible magnetization reversal, and  $H_{pulsed}$  is the pulsed field intensity and the angular distribution of magnetic moments  $P(\sigma, \Theta, \Phi)$ . To experimentally verify the proposed methodology, four magnets with different  $H_c$  values were used. Magnet 1  $H_c$  868 kAm, Magnet 2  $H_c$  1047 kAm, Magnet 3  $H_c$  1438 kAm and Magnet 4  $H_c$  1895 kAm. The

measured  $J_{r\_parallel}$  values and the  $J_{r\_perpendicular}$  values obtained using the proposed methodology allowed us to determine the degrees of alignment  $\cos\Theta_{star}$  for each magnet. From Magnet 1 to Magnet 4, these values were 973 percent, 977 percent, 881 percent and 948 percent, respectively. For comparison purposes, the degrees of alignment  $\cos\Theta$  were also calculated using the equation by Quispe et al 2020, yielding the following values from Magnet 1 to Magnet 4 976 percent, 990 percent, 900 percent and 998 percent. It is noted that for magnets with lower  $H_{cj}$  values, both approaches provide very similar  $\cos\Theta$  values. However, for magnets with higher  $H_{cj}$ , neglecting the effect of  $H_{cj}$  leads to an overestimation in the calculation of  $\cos\Theta$ , resulting in an absolute error of nearly 5 percent in the degree of alignment of Magnet 4. In magnets with even higher  $H_{cj}$  values, these errors may become more significant, emphasizing the importance of accounting for this effect.

**REFERENCES**[1] J. Magn. Magn. Mater. 382, 219–224 (2015).[2] J. Magn. Magn. Mater. 157–158, 19–20 (1996).[3] J. Appl. Phys. 128, (2020).[4] J. Magn. Magn. Mater. 612, 172639 (2024).

(Fig.1-a) Spatial distribution representation of magnetic moments of an NdFeB magnet

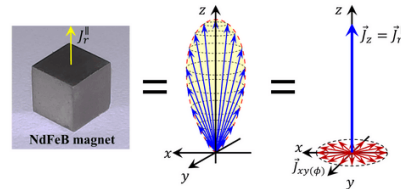
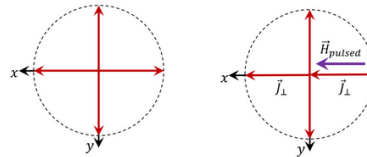
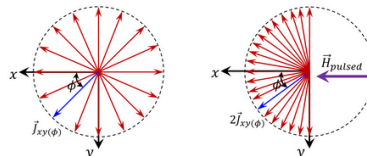


(Fig.1-b) Before (left) and after (right) magnetization in the direction perpendicular to the texture axis ( $\vec{H}_{pulsed} = H\hat{x}$ ), according to different approaches

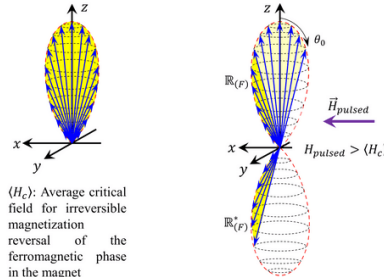
(i) W. Fernengel *et al.* (1996)



(ii) L. Quispe *et al.* (2020)



(iii) This work



📅 Mon. Jul 28, 2025 4:30 PM - 6:00 PM JST | Mon. Jul 28, 2025 7:30 AM - 9:00 AM UTC 🏠 Yellow zone, Conference rooms 101 and 102(1F)

## [P1] Processing, Characterization & Thin Films

Session Chair: Dr. Imants Dirba (Technical University of Darmstadt, Germany), Dr. Tae-Hoon Kim (Korea Institute of Materials Science, Korea)

### [P1-59] Temperature field variations during directional solidification of rare-earth large-size Tb-Dy-Fe magnetostrictive materials and their effect on growth orientation

\*jiang ping xin<sup>1</sup>, Jiheng Li<sup>1</sup>, Xiaoqian Bao<sup>1</sup>, Xuexu Gao<sup>1</sup> (1. USTB (China))

Keywords : magnetostriction、directed solidification、orientation、twinned crystals

Tb-Dy-Fe super magnetostrictive alloys are strongly anisotropic in magnetostrictive properties. The preparation of Tb-Dy-Fe alloys with highly axial selective orientation and high performance is of great research significance. Large-size Tb-Dy-Fe<110> oriented rod crystal materials are prepared by directional solidification technique. The temperature field derived from the finite volume method simulating the heat transfer during the directional solidification process shows that the temperature gradient at the solid-liquid interface front gradually decreases with the crystal growth, and the morphology of the mushy zone is transformed from a planar state to a concave state. The experiments show that as crystal growth proceeds, the grains grow along the heat flow direction, the main growth orientation is concentrated near the <110> direction, and the grains acquire the same organization as the direction of the easy magnetization axis through competitive growth, and the concentration of the <110> orientation decreases in the later stages of grain growth. On the one hand, the distribution of the temperature field in the late stage of directional solidification makes the state of the crystal growth front become concave, and there is an angle between the crystal growth direction and the axial direction; on the other hand, the reduction of the temperature gradient makes the supercooling degree of the grain growth front increase, and the increase of supercooling degree causes the change of the atomic stacking mode in the process of crystal growth, which is conducive to the creation of twins, and the creation of twins causes the crystal growth orientation to be changed. The twinning will change the orientation of the crystal growth.

📅 Mon. Jul 28, 2025 4:30 PM - 6:00 PM JST | Mon. Jul 28, 2025 7:30 AM - 9:00 AM UTC 🏠 Yellow zone, Conference rooms 101 and 102(1F)

## [P1] Processing, Characterization & Thin Films

Session Chair: Dr. Imants Dirba (Technical University of Darmstadt, Germany), Dr. Tae-Hoon Kim (Korea Institute of Materials Science, Korea)

### [P1-60] Bioinspired Design, Fabrication, and Wing Morphing of 3D-Printed Magnetic Butterflies

Muhammad Bilal Khan<sup>1</sup>, Kilan Schäfer<sup>1</sup>, Florian Hofmann<sup>1</sup>, Matthias Lutzi<sup>1</sup>, Eduardo Sergio Oliveros-Mata<sup>2</sup>, Oleksandr Pylypovskyi<sup>2</sup>, Denys Makarov<sup>2</sup>, \*Oliver Gutfleisch<sup>1</sup> (1. Functional Materials, TU Darmstadt (Germany), 2. Institute of Ion Beam Physics and Materials Research Helmholtz-Zentrum Dresden-Rossendorf e.V. (Germany))

Keywords : Additive Manufacturing、Magnetic Soft Robotics、Bioinspiration、Magnetic composites

Magnetic actuation enables fast, wireless, and safe operation of soft actuators (1,2). Additive manufacturing allows the creation of magneto-active composites in complex, bioinspired shapes (3). The impressive migratory capabilities of monarch butterflies, enabled by their efficient wing structures, serve as inspiration for bioinspired soft robots and microaerial vehicles. This study introduces the design, fabrication, and wing-morphing behavior of 3D-printed magnetic butterflies, emphasizing optimal material and design parameters to replicate the natural wing-morphing of monarchs (4). Using a composite of thermoplastic polyurethane and micron sized NdFeB magnetic powder, 12 distinct butterfly designs varying in size, vein patterns, and stiffness are produced through powder bed fusion (PBF) 3D printing, yielding a total of 84 specimens.

Deformation is induced in the specimens using a permanent magnet, effectively mimicking monarch butterflies without the need for embedded electronics. A combined approach of finite element simulations and experimental analysis explores how size, geometric features, and laser energy scale influence wing morphing. Lower laser energy scales produce porous specimens with rapid bending capabilities, while higher energy scales result in structures with greater mechanical strength and diverse deformation patterns. Additionally, vein structures enhance morphing performance.

This work was financially supported by the Deutsche Forschungs- gemeinschaft (DFG, German Research Foundation), Project ID No. 405553726, TRR 270, and the RTG 2761 LokoAssist (grant no. 450821862).

#### References

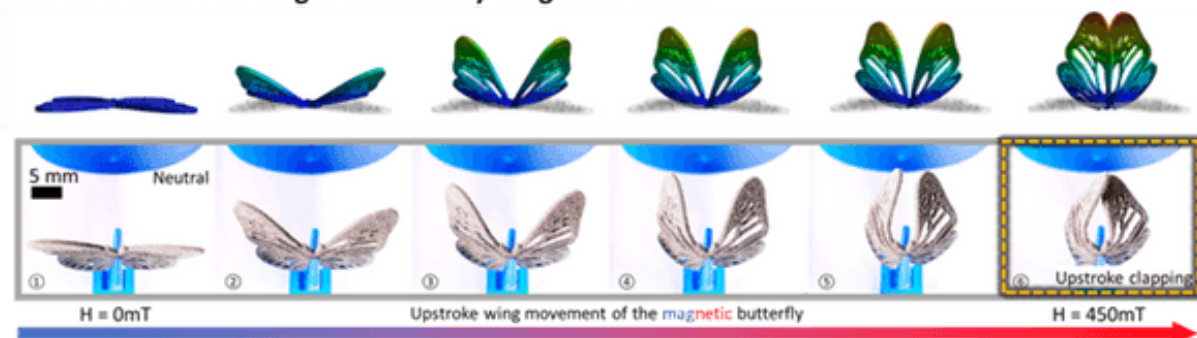
- (1) Y. Kim, X. Zhao, Chemical reviews, 2022, 122(5), 5317-5364.
- (2) X. Wang, G. Mao, J. Ge, M. Drack, ... D. Makarov, Communications Materials, 2020, 1(1), 67.
- (3) K. Schäfer, M. Lutzi, M.B. Khan, ... O. Gutfleisch, Additive Manufacturing, 2024, 79, 103905.
- (4) M.B. Khan, K. Schäfer, ... O. Gutfleisch, Advanced Intelligent Systems, 2024, 2400620.



### Wing-shape morphing behaviour of a Monarch butterfly



### Simulated and real magnetic butterfly wing movements



📅 Mon. Jul 28, 2025 4:30 PM - 6:00 PM JST | Mon. Jul 28, 2025 7:30 AM - 9:00 AM UTC 🏠 Yellow zone, Conference rooms 101 and 102(1F)

## [P1] Processing, Characterization & Thin Films

Session Chair: Dr. Imants Dirba (Technical University of Darmstadt, Germany), Dr. Tae-Hoon Kim (Korea Institute of Materials Science, Korea)

### [P1-61] Phase composition and magnetic properties of Nd(Pr)<sub>2</sub>Fe<sub>14</sub>B and (Sm,Zr)Fe<sub>11</sub>Ti magnets produced by selective laser melting

Sergey Andreev<sup>1</sup>, \*Viktoria Maltseva<sup>1</sup>, Dmitriy Neznakhin<sup>1</sup>, Arkadiy Shalaginov<sup>1</sup>, Andrey Urzhumtsev<sup>1</sup>, Alexey Volegov<sup>1</sup> (1. Ural Federal University (Russia))

Keywords : Additive manufacturing, Selective laser melting, Permanent magnets, Phase composition, Microstructure

Hard magnetic materials are classified among functional materials, which, in many respects, are the basis of modern technological processes, day-to-day operation devices, electrical transport, etc. The rate of improvement of the magnetic hysteretic properties of permanent magnets has steadily decreased because in the industrial production, the potential of the Nd<sub>2</sub>Fe<sub>14</sub>B compound has been realized almost completely. To further improve the functional properties of articles with permanent magnets, new approaches to designing such articles should be used. The additive manufacturing of functional magnetic materials and articles based on them is among these approaches. Additive technologies have several significant advantages over subtractive (edge cutting machining) and forming (strain without moving off a material) technologies. One of the advantages consists in the possibility of preparing samples and articles of any form, which is limited by the mechanical properties of a material. The other advantage is the local tuning of the material properties at the preparation stage at the expense of varying both the chemical composition and micro-structural state. In the present study, the effect of synthesis parameters on the phase composition and magnetic hysteretic properties of single-layer Nd<sub>2</sub>Fe<sub>14</sub>B-based permanent magnets synthesized by selective laser sintering is investigated. The causes for the effect of synthesis parameters on the magnetic hysteretic properties are considered. The possibility of reaching a coercivity of single-layer magnets of 19.5 kOe, which are free of heavy rare-earth metals, will be demonstrated. Also, this work presents a proof-of-concept of additive manufacturing of (Sm,Zr)Fe<sub>11</sub>Ti permanent magnet. A way to produce permanent magnets from (Sm,Zr)Fe<sub>11</sub>Ti powder and its mixture with low-melting additive Sm<sub>75</sub>(Cu, Co)<sub>25</sub> by the selective laser melting will be demonstrated. The phase transformations which accompany the liquid phase sintering of hard magnetic particles in low-melting Sm<sub>75</sub>(Cu,Co)<sub>25</sub> additive will be discussed. The printing parameters which allow sintering of the hard magnetic alloy particles were found. When the main phase is (Sm,Zr) Fe<sub>11</sub>Ti, the coercivity of  $H_c = 5$  kOe is achieved. This work was financially supported by FEUZ-2024-0066.

📅 Mon. Jul 28, 2025 4:30 PM - 6:00 PM JST | Mon. Jul 28, 2025 7:30 AM - 9:00 AM UTC 🏠 Yellow zone, Conference rooms 101 and 102(1F)

## [P1] Processing, Characterization & Thin Films

Session Chair: Dr. Imants Dirba (Technical University of Darmstadt, Germany), Dr. Tae-Hoon Kim (Korea Institute of Materials Science, Korea)

### [P1-62] Grain alignment by single track printing using anisotropic sintered Nd-Fe-B magnet as a substrate

Peishu Song<sup>1</sup>, Zhenyuan Liu<sup>1</sup>, Yan Li<sup>2</sup>, Dan Han<sup>3</sup>, \*Lanting Zhang<sup>1</sup> (1. Shanghai Jiao Tong University (China), 2. Inner Mongolia University of Science and Technology (China), 3. Inner Mongolia Research Institute of Shanghai Jiao Tong University (China))

Keywords : Selective laser melting、Nd-Fe-B、<001> orientation、melt pool、dendrite growth

The relatively high cooling rate during SLM is likely to suppress the formation of  $\alpha$ -Fe and allow designed composition distribution in the magnet which is beneficial to the magnetic properties. Many works have devoted to the effects of printing parameters on grain size, phase transition and magnetic properties of printed magnets[1]. Wu et al[2] presented an in-depth analysis on grain structure of the SLM magnet for the first time in terms of morphology, size distribution, and texture. The formation and transformation mechanisms of complex phases and the development of nanocrystalline microstructures during the SLM process were investigated. Huber et al[3] reported that it was confirmed that the coercive force increased by infiltrating the low melting point rare earth eutectic alloy into the Nd-Fe-B magnet fabricated by LPBF. However, current works are predominantly focused on optimizing the printing parameters to enhance the coercivity of magnets, with scant attention given to the enhancement of grain orientation in SLM processed Nd-Fe-B magnets. the present study explores the impact of utilizing an anisotropic sintered Nd-Fe-B magnets as a substrate to induce orientated grains and desired microstructure of the magnets after SLM.

Spherical Nd-Fe-B commercial powder (MQP-S-11-9-20001) from Magnequench with an average size of 43  $\mu\text{m}$  and a composition of  $\text{Nd}_{17.2}\text{Pr}_{1.9}\text{Fe}_{69.8}\text{Co}_{2.8}\text{Ti}_{2.1}\text{Zr}_{4.3}\text{B}_{1.7}$  (wt%) was used. An N52-grade commercial sintered magnet ( $\text{Nd}_{29}\text{Fe}_{61}\text{Co}_{1.5}\text{B}_{0.99}\text{Cu}_{0.17}\text{Ga}_{0.1}\text{Ti}_{0.18}$  (wt%)) was employed as the substrate. SLM equipment applied was Truprint 1000 equipped with a 200 W Yb: YAG pulsed fiber laser (spot size: was 30  $\mu\text{m}$ ). The laser power P and scanning speed V attempted in the present work varied from 80 W to 200W and from 20 mm/s to 800 mm/s using fixed layer thickness of 30  $\mu\text{m}$  of the powder. The distance between the adjacent single tracks is set to 2 mm and the dimension of the Nd-Fe-B substrate magnet was  $25 \times 10 \times 5 \text{ mm}^3$ , with its easy magnetization axis (c-axis) parallel to the building direction. Optical microscopy (OM) was used to observe the surface morphology of the single tracks after SLM. The melt pools and cross sections of the tracks were observed by a scanning electron microscope (SEM). The orientation of the grains in the melt pool was characterized by electron backscatter diffraction (EBSD) operated at 20 kV.

As shown in Figure 1, The cross section of the melt pool after solidification can be broadly

classified into four regions: the dendritic zone, the equiaxed fine grain region, the heat-affected zone and the un-melted substrate region. The area fraction of the dendritic region increases with increasing line energy density ( $E_L$ ). The majority of the grains in the melt pool (140W, 50mm/s,  $E_L=2.8$  J/mm) are  $\langle 001 \rangle$  orientated which aligns with that of the substrate magnet. Only a small portion of the initially grown grains at the edge of the melt pool (140W, 200mm/s,  $E_L=0.7$  J/mm) keep the same orientation as the substrate grains. The width and depth of the melt pool under 140 W, 50 mm/s ( $\sim 500$   $\mu\text{m}$  wide and  $\sim 400$   $\mu\text{m}$  deep) are larger than that those under 140 W, 200 mm/s ( $\sim 320$   $\mu\text{m}$  wide and  $\sim 210$   $\mu\text{m}$  deep). A sufficient growth of the dendrite zone is crucial to form the orientated grains with the same orientation as the substrate.

In the direct laser remelting process, a slow scanning speed of 20 mm/s ( $E_L=7$  J/mm) is favorable to form  $\langle 001 \rangle$  orientated grains than 200 mm/s ( $E_L=0.7$  J/mm) under 140 W laser power. In the SLMed single track study,  $\langle 001 \rangle$  orientated Nd-Fe-B grains are formed in the dendrite zone under the  $E_L = 2.8$  J/mm. The grains in the MP-fine zone are randomly orientated. It confirmed the feasibility of using anisotropic sintered Nd-Fe-B magnet as the substrates to enhance the orientation of SLMed magnet.

## References

- [1] B. Yao et al. International Journal of Extreme Manufacturing 6(1) (2024) 015002.
- [2] J. Wu et al. Acta Materialia 259 (2023) 119239.
- [3] C. Huber et al. Acta Materialia 172 (2019) 66-71.

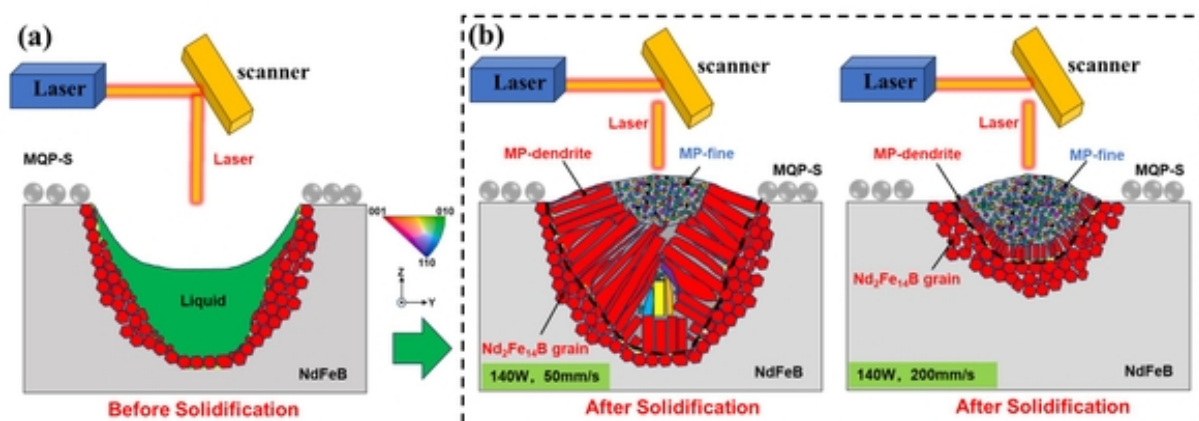


Figure 1. Schematic of melt pool morphology and grain growth of Nd-Fe-B magnet (a) before and (b) after solidification during the SLM process

📅 Mon. Jul 28, 2025 4:30 PM - 6:00 PM JST | Mon. Jul 28, 2025 7:30 AM - 9:00 AM UTC 🏢 Yellow zone, Conference rooms 101 and 102(1F)

## [P1] Processing, Characterization & Thin Films

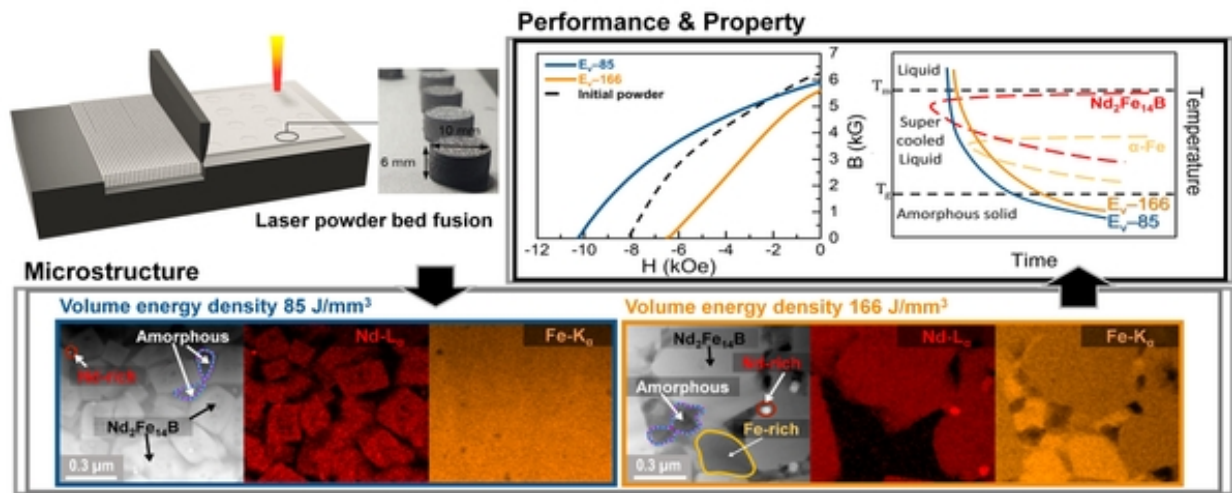
Session Chair: Dr. Imants Dirba (Technical University of Darmstadt, Germany), Dr. Tae-Hoon Kim (Korea Institute of Materials Science, Korea)

### [P1-63] Microstructural Investigation of Nd-Fe-B Magnets Fabricated by Laser Powder Bed Fusion

\*Hojeong Kim<sup>1</sup>, Taesuk Jang<sup>2</sup>, Du-Rim Eo<sup>3</sup>, Wooyoung Lee<sup>1</sup> (1. Yonsei university (Korea), 2. Sunmoon University (Korea), 3. KITECH (Korea))

Keywords : Additive manufacturing、Nd-Fe-B、Permanent magnet、Laser powder bed fusion、Solidification、Amorphous phase

Nd-Fe-B magnets were manufactured by laser powder bed fusion (LPBF) using commercially available spherical powder (MQP-S-11-9). The magnets were manufactured at four different volume energy densities but similar relative densities to investigate the relations between the process, structure, and characteristics. Unlike the nanocomposite microstructure of the initial powder, the microstructure of the LPBF samples had (Nd, Pr)<sub>2</sub>Fe<sub>14</sub>B grains separated by grain boundary phases through the remelting and solidification of the initial powder. The cooling rate of the melt pool increased as the volume energy density decreased, suppressing the crystallization of  $\alpha$ -Fe in the grain boundary phase. When the volume energy density was less than 86 J/mm<sup>3</sup>, the crystallization of  $\alpha$ -Fe was fully suppressed, and the grain boundary phases became amorphous, resulting in higher coercivity than that of the initial powder. The magnet with the strongest magnetic properties of  $H_{ci} = 10.3$  kOe,  $B_r = 6.2$  kG, and  $(BH)_{max} = 7.5$  MGOe was produced when LPBF was performed under the conditions of P90, V500, H70, and L30 (volume energy density = 85.7 J/mm<sup>3</sup>). The solidification behavior of Nd-Fe-B magnets during LPBF was analyzed in detail using thermodynamic simulations. In this study, the microstructure of the fusion zone (FZ) and the heat affected zone (HAZ) according to process parameters was analyzed, and the effect of the solidification microstructure on the magnetic properties of Nd-Fe-B magnets was reported.



📅 Mon. Jul 28, 2025 4:30 PM - 6:00 PM JST | Mon. Jul 28, 2025 7:30 AM - 9:00 AM UTC 🏠 Yellow zone, Conference rooms 101 and 102(1F)

## [P1] Processing, Characterization & Thin Films

Session Chair: Dr. Imants Dirba (Technical University of Darmstadt, Germany), Dr. Tae-Hoon Kim (Korea Institute of Materials Science, Korea)

### [P1-64] From Scrap to Bonded Magnet: Exploring Nanocrystalline Recycled Powders in Additive Manufacturing

\*Marcelo Augusto Rosa<sup>1</sup>, Gabriel Maia<sup>2</sup>, Apuniano Baldarrago<sup>1</sup>, Maximiliano Martins<sup>2</sup>, Paulo Wendhausen<sup>1</sup> (1. UFSC (Brazil), 2. CDTN (Brazil))

Keywords : additive manufacturing、fused deposition modelling、recycling、bonded magnet

Bonded Nd-Fe-B magnets are usually fabricated by blending magnetic powders with polymeric binders to facilitate shaping via compression or injection moulding. In recent years, Additive Manufacturing (AM) has been envisaged as a complementary method, due to the possibility of obtaining complex shapes and field configurations without using any mould (1,2). Different AM techniques were explored, mainly Laser Powder Bed Fusion (LPBF), but also Fused Deposition Modelling (FDM), and Stereolithography (SLA) (3,4). The common practice is using commercial powders for that purpose. However, as far as we know, the preparation of AM feedstocks from end-of-life magnets and their use in AM has not been thoroughly addressed, which is the main proposal of this work. Our primary objective is to investigate the fabrication of bonded magnets via AM, using feedstocks composed of nanocrystalline powders obtained from scrap. Recycling has been gaining momentum and most efforts have aimed to obtain sintered magnets via the magnet-to-magnet approach. Reprocessing means pickup of oxygen, leading to a depletion of the Nd-rich phase, which plays a pivotal role in guaranteeing high density and high coercivity in the recycled magnets. But recycling strategies can be rethought towards the fabrication of bonded magnets instead of sintered ones. The scenario is different for bonded magnets because densification is driven by a binder, and high coercivity can be assured by grain refinement techniques, such as the hydrogenation-disproportionation-desorption-recombination (HDDR) process (5). Previous contributions have addressed the use of nanocrystalline recycled powders in the fabrication of bonded magnets using conventional shaping processes. Our contribution focuses on AM processing, more specifically the FDM technique. Nd-Fe-B N35 scrap magnets were subjected to hydrogen processing to obtain nanocrystalline powders. Hydrogen decrepitation (HD) was performed, and then the HD powder was transferred to a glovebox under inert conditions, where it was milled (mortar) and sieved to a particle size  $<63\text{ }\mu\text{m}$ . Milling was performed to adequate particle size for AM purposes. Laser diffraction analyses revealed a mean particle size of  $(29\pm5)\text{ }\mu\text{m}$  for the HD powder. Afterwards, the HD powder was processed via conventional HDDR, which resulted in isotropic particles with mean values of coercivity equal to  $(750\pm75)\text{ kA/m}$  and remanence of  $(705\pm14)\text{ mT}$ . The HDDR powder was also transferred to the glovebox and milled  $<63\text{ }\mu\text{m}$ . According to laser diffraction characterization, the nanocrystalline powders presented an average particle diameter of

(50+-32)  $\mu\text{m}$ . The grain size was assessed by analysing SEM images, revealing an average diameter of (195+-68) nm. To prepare the feedstock for FDM, the nanocrystalline recycled powder was mixed with polylactic acid (PLA) pellets with different vol. fractions of powder (from 5% up to 60%) using a hot mixer setup, where pellets and the powder were heated under vacuum up to 170 °C and then mixed for 30 min. The feasibility of producing filaments for FDM was then explored for each mixture, and it was possible to obtain filaments containing up to 50% in vol. of magnetic load. Such filaments were used to 3D print bonded magnets, reaching average coercivity of (685 $\pm$ 21) kA/m. The present work has demonstrated the obtention of ready-to-use AM feedstock for FDM starting from scrap magnets, including the obtention of complex-shape bonded magnets, which may open a variety of new possible applications. The next steps include exploring strategies to increase even further the magnetic load in the filaments and also to develop in situ aligning systems to obtain anisotropic bonded magnets. References: (1) A. Baldissera, et. al. IEEE International Magnetism Conference (INTERMAG), 2017. p. 1. (2) M. Parans Paranthaman, et. al. The Journal of The Minerals, Metals & Materials Society, 2016. vol. 68, no. 7. (3) R.G.T. Fim, et. al. Additive Manufacturing, 2020. vol. 35, 101353. (4) G. Maia, et. al. Ready to use Composite FDM Filaments produced with PLA and Recycled NdFeB Nanocrystalline Powder for additive manufacturing of bonded magnets. Accepted Manuscript, IEEE Magnetism Letters, 2025. (5) M.A. Rosa, et. al. IEEE International Magnetism Conference (INTERMAG), 2024. vol. 60, issue 9, 2100805.



📅 Mon. Jul 28, 2025 4:30 PM - 6:00 PM JST | Mon. Jul 28, 2025 7:30 AM - 9:00 AM UTC 🏠 Yellow zone, Conference rooms 101 and 102(1F)

## [P1] Processing, Characterization & Thin Films

Session Chair: Dr. Imants Dirba (Technical University of Darmstadt, Germany), Dr. Tae-Hoon Kim (Korea Institute of Materials Science, Korea)

### [P1-65] Enhancing the Printability of Nd-Fe-B Feedstocks for Laser Powder Bed Fusion

Marcelo Augusto Rosa<sup>1</sup>, Apuniano Baldarrago<sup>1</sup>, Arthur Mascheroni<sup>2</sup>, José Maria Mascheroni<sup>2</sup>, \*Paulo Wendhausen<sup>1</sup> (1. UFSC (Brazil), 2. Alkimat (Brazil))

Keywords : additive manufacturing、laser powder bed fusion、feedstock、bonded magnet

Over the past decade, Additive Manufacturing (AM) has emerged as a complementary method for producing bonded magnets. Among the various AM techniques, Laser Powder Bed Fusion (LPBF) has shown significant potential, achieving dense bonded magnets with a volume fraction of magnetic particles around 50% vol (1,2). Other techniques such as Fused Deposition Modelling (FDM) were also explored, but in this case, a magnetic load no higher than 22% were obtained (3). In the end, a bonded magnet with high coercivity and high remanence is desired. The coercivity depends fundamentally on the kind of magnetic powder used to compose the feedstock, so it is a fixed parameter (considering that no degradation of the magnetic particles takes place during additive manufacturing). Remanence, on the other hand, depends on particle alignment and the vol. fraction of magnetic particles (4,5). To date, most of the research has concentrated on changing printing parameters to enhance especially the magnetic load of printed magnets. The strategies adopted consisted of optimizing laser processing parameters (scanning speed, hatch space, etc) to eliminate pores and improve the magnetic load. In contrast, this study shifts the focus towards the preparation of feedstocks with enhanced technological properties, specifically targeting the flowability of the particles, the overall magnetic load of the feedstock, its apparent density, and composite particle morphology. These properties collectively contribute to what the literature refers to as printability. The experimental methodology involves the preparation of magnetic powder from end-of-life magnets through hydrogen processing, which includes hydrogen decrepitation followed by the hydrogenation-disproportionation-desorption-recombination process, with the objective of obtaining a coercive powder. Powders with mean coercivities of 737 kA/m were obtained. The resulting powder is then combined with various binders such as PA12, PLA, and PP, in different volume fractions, using a hot mixing technique. The composite chips thus obtained are produced under vacuum conditions using a Winkworth hot blender, with working temperatures exceeding 150°C, depending on the binder used. Subsequently, the composite chips are milled in a knife mill and processed in Alkimat for particle spheroidization. A notable distinction in this approach is the preparation of composite particles, wherein the magnetic particles are embedded within a polymeric matrix, as confirmed by SEM analysis. This contrasts with previous studies where feedstocks were prepared through simple mechanical mixing under room conditions, resulting in a blend of separate magnetic and binder particles. The composite approach

offers several advantages, including the prevention of phase segregation—often observed due to density differences between polymeric and metallic particles—and the ability to leverage the processability of the binder to spheroidize the composite particles, thereby enhancing flowability during printing. For polypropylene-based feedstocks, a magnetic load of up to 60% vol. was achieved. Comprehensive evaluations were conducted on all types of feedstocks in terms of flowability, magnetic load, and printability. The findings demonstrate that the preparation of feedstocks with improved technological properties not only enhances the performance of bonded magnets but also offers a novel approach to optimizing the LPBF process. This study paves the way for future research and development in the field of AM for bonded magnets, emphasizing the critical role of feedstock preparation in achieving superior magnet performance. Notably, the most promising results were obtained using polypropylene-based feedstocks, for which the magnetic load was increased to 55% vol. (1) A. Baldissera, et. al. IEEE International Magnetism Conference (INTERMAG), 2017. p. 1. (2) R.G.T. Fim, et. al. Additive Manufacturing, 2020. vol. 35, 101353. (3) G. Maia, et. al. Ready to use Composite FDM Filaments produced with PLA and Recycled NdFeB Nanocrystalline Powder for additive manufacturing of bonded magnets. Accepted Manuscript, IEEE Magnetism Letters, 2025. (4) M.C. Mapley, et al. Selective laser sintering of bonded anisotropic permanent magnets using an in situ alignment fixture, Rapid Prototyping Journal, vol. 27, no. 4, p. 735 740. (5) K. Schafer, et. al. Laser powder bed fusion of anisotropic Nd Fe B bonded magnets utilizing an in situ mechanical alignment approach. Journal of Magnetism and Magnetic Materials, 2023. vol. 583, 171064.

📅 Mon. Jul 28, 2025 4:30 PM - 6:00 PM JST | Mon. Jul 28, 2025 7:30 AM - 9:00 AM UTC 🏠 Yellow zone, Conference rooms 101 and 102(1F)

## [P1] Processing, Characterization & Thin Films

Session Chair: Dr. Imants Dirba (Technical University of Darmstadt, Germany), Dr. Tae-Hoon Kim (Korea Institute of Materials Science, Korea)

### [P1-66] Preparation of micromagnets via LIFT technique

\*Masaki Nakano<sup>1</sup>, Gakuto Tahara<sup>1</sup>, Takuki Amiya<sup>1</sup>, Akihiro Yamashita<sup>1</sup>, Takeshi Yanai<sup>1</sup>, Masaru Itakura<sup>2</sup>, Kunihiro Koike<sup>3</sup>, Hirotohi Fukunaga<sup>1</sup> (1. Nagasaki university (Japan), 2. Kyushu university (Japan), 3. Yamagata university (Japan))

Keywords : micromagnets、LIFT technique、PLD method

Although our group has focused on the fabrication of rare-earth film magnets using a Pulsed Laser Deposition method <sup>[1]</sup>, these samples require high-temperature heat treatment above 723 K, such as substrate heating or post-annealing, to obtain hard magnetic properties. At present, film magnets are expected to be used in MEMS, and a fabrication method employing lower temperatures is required to facilitate compatibility with other devices and low-melting-point materials in MEMS. Recently, we prepared Nd-Fe-B film magnets fabricated by the aforementioned PLD as donors and successfully prepared Nd-Fe-B micromagnets using a Laser Induced Forward Transfer technique <sup>[2]</sup>. In the technique, a specimen is prepared on a laser-transparent glass substrate, subsequently subjected to heat treatment, and irradiated by a laser from the donor side, resulting in the deposition of a transfer film on the receiver substrate. However, the coercivity of current micromagnets is only approximately 200 kA/m <sup>[2]</sup> compared to the coercivity of the donor exceeding 200 kA/m. In this study, we report the effects of energy density in the LIFT technique on the coercivity of Nd-Fe-B micromagnets of various thicknesses. Nd-Fe-B micromagnets were deposited in a high vacuum using a YAG laser with a wavelength of 355 nm and a repetition rate of 30 Hz. NdFe-B film magnets fabricated by PLD were used as donors, and Ta substrates were used as receivers. In this experiment, the energy density of the laser beam was controlled by the spot size and power of the laser. Figure 1 illustrates the comparison of the coercivity values between donors and receivers by modulating the laser energy density in relation to the donor film thickness. A correlation between the coercivity of the donor and receiver was observed for the ratio of film-thickness to energy-density between 4 and 9 microns/(J/cm<sup>2</sup>). Micromagnets with coercivity of approximately 500 kA/m could be obtained through modulation of the energy density, representing a significant enhancement over the previously reported maximum value <sup>[2]</sup>. X-ray diffraction patterns of the two samples prepared with varying thickness-to-energy density ratios were observed. Under optimal conditions, a prominent Nd<sub>2</sub>Fe<sub>14</sub>B phase was observed, whereas the α-Fe peak was suppressed. These findings suggest that the previously reported inability to achieve improved coercivity may be attributed to the application of suboptimal laser energy density for a given film thickness. References [1]Nakano *et al.*, IEEE Trans. Magn., **56**, (2020) #7516303. [2]Nakano *et al.*, IEEE Trans. Magn., **60**, (2024) #2100604.

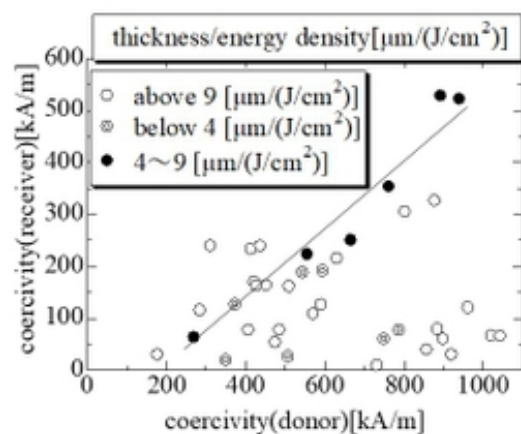


Figure 1. Relationship between coercivity of donor and receiver for varying film thicknesses and laser energy densities.

📅 Mon. Jul 28, 2025 4:30 PM - 6:00 PM JST | Mon. Jul 28, 2025 7:30 AM - 9:00 AM UTC 🏠 Yellow zone, Conference rooms 101 and 102(1F)

## [P1] Processing, Characterization & Thin Films

Session Chair: Dr. Imants Dirba (Technical University of Darmstadt, Germany), Dr. Tae-Hoon Kim (Korea Institute of Materials Science, Korea)

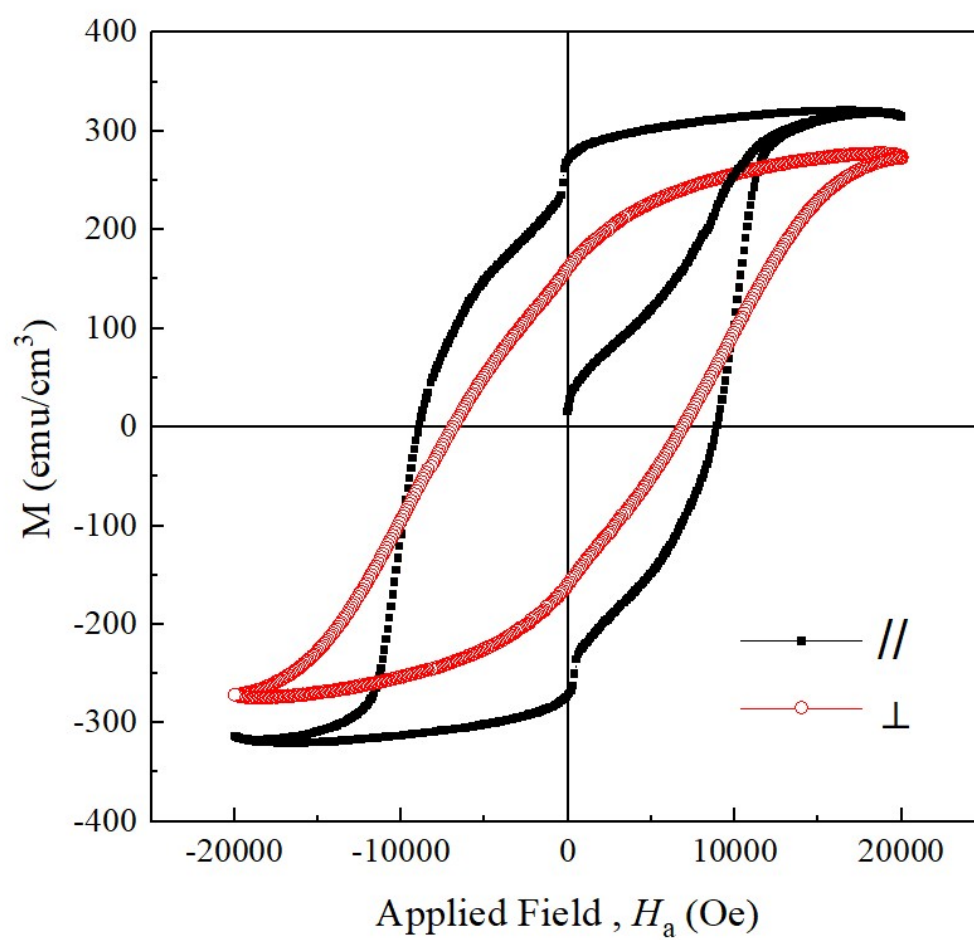
### [P1-67] Sputtered high-coercivity CeCo thin film on glass substrate

Cheng-Yan Lee<sup>2</sup>, Sea-Fue Wang<sup>2</sup>, Huang-Wei Chang<sup>3</sup>, \*An-Cheng Aidan Sun<sup>1</sup> (1. Yuan Ze University (Taiwan), 2. National Taipei University of Technology (Taiwan), 3. National Chung Cheng University (Taiwan))

Keywords : CeCo, Thin Film, Magnetic

CeCo permanent magnetic materials have been widely studied in bulk, powder, and ribbon forms. However, their thin-film counterparts remain relatively unexplored. To expand the application of CeCo permanent magnetic materials in MEMS, sensors, and magnetic recording devices, it is essential to develop CeCo thin films with optimized magnetic properties. Sputtering is a promising fabrication method due to its compatibility with mass production and ability to produce thin films with high coercivity and magnetization. However, reports on the successful sputtering of CeCo thin films with high magnetic performance remain limited.

In this study, high-coercivity CeCo thin films were deposited on glass substrates using a sputtering system with a CeCo alloy target. The base pressure was maintained below  $5 \times 10^{-7}$  Torr, and the argon working pressure was set at 10 mTorr. The thin films were deposited at room temperature using RF sputtering at 100 W, followed by rapid thermal annealing at 400°C for 10 minutes. The phase structure and magnetic properties were analyzed using X-ray diffraction (XRD) and vibrating sample magnetometry (VSM). The results confirmed that the CeCo thin films exhibited high coercivity in both in-plane ( $H_{c//} = 9000$  Oe) and out-of-plane ( $H_{c\perp} = 7000$  Oe) directions, along with a saturated magnetization ( $M_s$ ) of approximately  $320 \text{ emu/cm}^3$ . The initial magnetization curve indicated that coercivity was initially dominated by domain wall motion, followed by a combination of domain wall motion and rotation mechanisms. Additionally, the shoulder-like feature near the zero-field range suggested the presence of a minor soft magnetic phase, likely due to insufficient thermal energy during the annealing process. Future investigations will focus on further characterizing the microstructure and magnetic properties of sputtered CeCo thin films to optimize their performance for potential applications.



Poster | Material, processing, and characterization

📅 Mon. Jul 28, 2025 4:30 PM - 6:00 PM JST | Mon. Jul 28, 2025 7:30 AM - 9:00 AM UTC 🏢 Yellow zone, Conference rooms 101 and 102(1F)

## [P1] Processing, Characterization & Thin Films

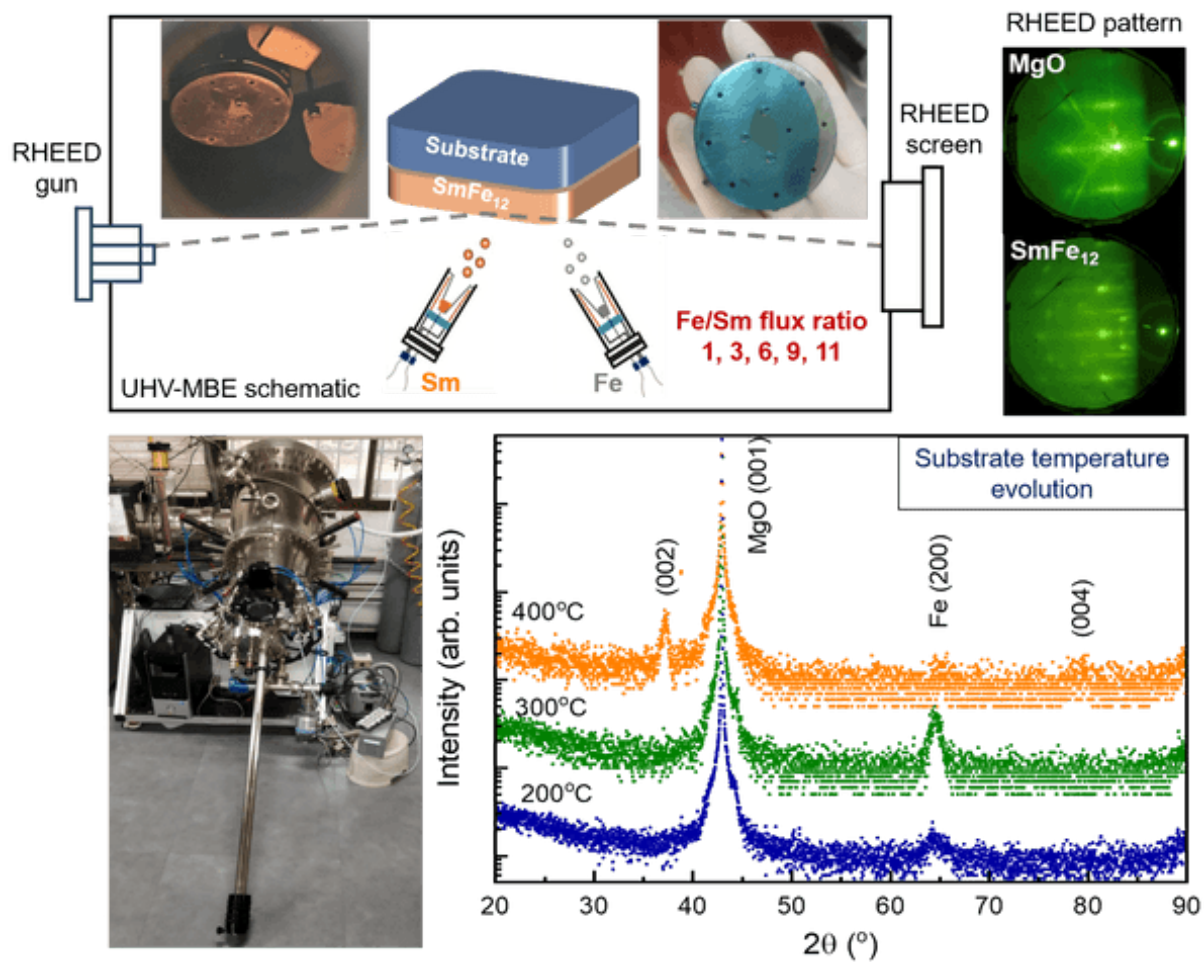
Session Chair: Dr. Imants Dirba (Technical University of Darmstadt, Germany), Dr. Tae-Hoon Kim (Korea Institute of Materials Science, Korea)

### [P1-68] Growth of SmFe<sub>12</sub> thin films using MBE

\*Uyanga Enkhnanan<sup>1</sup>, Jargalan Narmandakh<sup>1</sup>, Sangaa Deleg<sup>1</sup>, Uranbaigal Enkhtur<sup>2</sup>, Odkhuu Dorj<sup>2</sup>, Sunglae Cho<sup>3</sup> (1. Institute of Physics and Technology of Mongolian Academy of Sciences (Mongolia), 2. Incheon National University (Korea), 3. University of Ulsan (Korea))

Keywords : SmFe<sub>12</sub> thin film、 Molecular Beam Epitaxy

ThMn<sub>12</sub>-ordered SmFe<sub>12</sub> has been considered one of the most promising candidates as a competitive alternative to state-of-the-art permanent magnets. In this study, SmFe<sub>12</sub>/Fe (001) composite thin films with high extrinsic coercivity were successfully demonstrated. The films were grown using molecular beam epitaxy (MBE), with systematic variation of Sm and Fe flux ratios to optimize their magnetic and structural properties for high-performance applications. For Sm-rich films, a c-axis textured SmFe<sub>12</sub> structure with in-plane magnetization was achieved. An exceptionally high coercivity of 0.44 T was observed at an Fe/Sm ratio of 6, attributed to the formation of intergranular phases that enhance magnetic stability. The growth of SmFe<sub>12</sub> thin films on MgO (100) using MBE was investigated, with the experimental setup including an MBE schematic, RHEED patterns, and XRD profiles highlighting the temperature dependence, as shown in the following schematic figure.





📅 Mon. Jul 28, 2025 4:30 PM - 6:00 PM JST | Mon. Jul 28, 2025 7:30 AM - 9:00 AM UTC 🏠 Yellow zone, Conference rooms 101 and 102(1F)

## [P1] Processing, Characterization & Thin Films

Session Chair: Dr. Imants Dirba (Technical University of Darmstadt, Germany), Dr. Tae-Hoon Kim (Korea Institute of Materials Science, Korea)

### [P1-69] Development of data handling tools for high-throughput experiments

\*Pierre Le Berre<sup>1</sup>, William Rigaut<sup>1</sup>, Wilfried Hortschitz<sup>2</sup>, Santa Pile<sup>2</sup>, Harald Oezelt<sup>2</sup>, Samuel J. R. Holt<sup>3,4</sup>, Swapneel A. Pathak<sup>3,4</sup>, Hans Fangohr<sup>3,4,5</sup>, Thomas Schrefl<sup>2</sup>, Thibaut Devillers<sup>1</sup>, Nora M. Dempsey<sup>1</sup> (1. Univ. Grenoble Alpes, CNRS, Grenoble INP, Institut Néel, 38000 Grenoble (France), 2. Department for Integrated Sensor Systems, University for Continuing Education Krems, Wr. Neustadt (Austria), 3. Max Planck Institute for the Structure and Dynamics of Matter, Luruper Chaussee 149, 22761 Hamburg (Germany), 4. Center for Free-Electron Laser Science, Luruper Chaussee 149, 22761 Hamburg (Germany), 5. Faculty of Engineering and Physical Sciences, University of Southampton, Southampton SO17 1BJ (UK))  
Keywords : high-throughput, data, thin films, combinatorial

Over the last decades, the combinatorial approach to the exploration of material systems has garnered great interest as a novel way to efficiently optimize functional materials [1]. High-throughput characterization techniques can quickly generate huge amounts of data which needs to be sorted, analyzed and stored, both for human exploitation and for use as input in machine learning models. At Institut Néel, a thin-film based combinatorial approach is being developed to study the effects of elemental substitution and processing conditions on different hard magnetic material systems. Specific software tools have been developed to handle the data sets generated by Energy Dispersive X-Ray (EDX) spectroscopy, mechanical profilometry, X-Ray Diffraction (XRD), Magneto-Optic Kerr effect (MOKE) magnetometry and Scanning Electron Microscopy. To deal with the data, we have created an HDF5 based file system which is particularly suited to handle multi-dimensional datasets, such as those found in combinatorial material science. These files ensure generated data is traceable, convenient to store and easy to share. The file system is integrated with the Magnetic Material Ontology [2] and aggregates within a single file all relevant metadata, raw data and analysis results from a battery of different instruments and measurements. These files also serve as a digital log, recording all the stages of a sample's life with all the necessary information, including user notes. To generate and interface with the HDF5 files, a software suite has been developed, based on Python and Plotly-Dash [3]. The software allows for quick visualization of complex datasets, so that users can evaluate the quality of generated datasets, and it also allows for the customizable export of datasets in a format that can then be used as input in machine learning models. All of this work is open-source and can be expanded on for use with different experimental setups, in an effort to push towards traceable, shareable data.

[1] ML Green et al., J. Appl. Phys. 113 (2013) 231101

[2] [https://mammos-project.github.io/MagneticMaterialsOntology/doc/magnetic\\_material\\_mammos.html](https://mammos-project.github.io/MagneticMaterialsOntology/doc/magnetic_material_mammos.html)

[3] <https://plotly.com/>

Acknowledgements: This work is being carried out within the framework of the EU funded

MaMMoS project (Grant number 101135546, HORIZON-CL4-2023-DIGITAL-EMERGING-01), the ANR-FWF funded DATAMAG project (ANR-22-CE91-0008 / FWF I 6159-N) and the ANR/DIADEM MIAM project (ANR-23-PEXD-0013).

📅 Mon. Jul 28, 2025 4:30 PM - 6:00 PM JST | Mon. Jul 28, 2025 7:30 AM - 9:00 AM UTC 🏠 Yellow zone, Conference rooms 101 and 102(1F)

## [P1] Processing, Characterization & Thin Films

Session Chair: Dr. Imants Dirba (Technical University of Darmstadt, Germany), Dr. Tae-Hoon Kim (Korea Institute of Materials Science, Korea)

### [P1-70] Towards the high-throughput microstructural characterisation of compositionally graded NdFeB-based films

\*Lukas Fink<sup>1</sup>, William Rigaut<sup>1</sup>, Pierre Le-Berre<sup>1</sup>, Heisam Moustafa<sup>2</sup>, Qais Ali<sup>2</sup>, Leoni Breth<sup>2</sup>, Thomas Schrefl<sup>2</sup>, Harald Oezelt<sup>2</sup>, Thibaut Devillers<sup>1</sup>, Nora M. Dempsey<sup>1</sup> (1. 1Université Grenoble Alpes, CNRS, Grenoble INP, Institut Néel, 38000 Grenoble (France), 2. Department for Integrated Sensor Systems, University for Continuing Education Krems, 2700 Wr. Neustadt (Austria))

Keywords : High-throughput characterisation, Thin film, Microstructure

In the ongoing efforts to reduce CO<sub>2</sub> emissions, there has been a drastic increase in the utilisation of environmentally sustainable technologies for power generation and transportation. Nevertheless, the prevailing reliance on magnetic materials poses a considerable challenge since these materials are composed of rare earth and cobalt, among other critical elements. Therefore, the objective is to identify novel magnetic materials that can match the properties of existing materials while demonstrating superior environmental and economic viability. Achieving this goal requires screening a vast number of materials, but conventional methods limit exploration to compositions near known materials. A promising approach is combinatorial studies based on the preparation of compositionally graded films [1]. These enable efficient screening and optimisation of functional materials, through the use of high throughput characterization methods. In the case of hard magnetic FePt [2] and NdFeB-based [3] films, high-throughput characterization made it possible to systematically analyse the extrinsic magnetic properties, the chemical composition and the crystal structure, enabling the correlation of trends and identification of causal relationships. However, variations in microstructure have not been considered in these investigations. This is of particular relevance, given the established influence of microstructure on the extrinsic magnetic properties of hard magnetic materials.

In this study, we establish a high-throughput methodology for microstructural characterisation of NdFeB-based films, using argon Ion Beam Etching (IBE) followed by plan-view Scanning Electron Microscopy (SEM) imaging. The etching step is used to fully remove the protective 10 nm Ta capping layer, and to partially remove material from the upper surface of the NdFeB-based film. The prominence of the revealed microstructural features depends of the duration of etching (Fig. 1). After 10 minutes of etching, the grain structure of the main 2:14:1 phase is discernible through the presence of voids, known to form in such films [4]. After 25 minutes of etching, individual grains of the main 2:14:1 phase can be clearly distinguished, thanks to preferential etching of the rare earth rich secondary phases. The latter type of images are well suited to grain size distribution analysis. By automating wafer-level SEM imaging and image analysis across

compositionally graded films, we can map the lateral distribution of different microstructural features. This can then contribute to establishing correlations between structural and magnetic properties, through machine learning analysis and micromagnetic modelling [5]. This approach enhances the efficiency of combinatorial materials screening, providing deeper insights into structure-property relationships critical for next-generation magnetic materials.

- [1] ML Green et al., *J. Appl. Phys.* 113 (2013) 231101
- [2] Y. Hong et al., *J. Mater. Res. Technol.* 18 (2022) 1245
- [3] A. Kovacs et al., *Front. Mater* 9 (2023) 1094055
- [4] N.M. Dempsey et al., *Acta. Mat.* 61 (2013) 4920
- [5] H. Moustafa et al., *AIP Advances* 14 (2024) 025001

Acknowledgements: This work is being carried out within the framework of the EU funded MaMMoS project (Grant number 101135546, HORIZON-CL4-2023-DIGITAL-EMERGING-01), the ANR-FWF funded DATAMAG project (ANR-22-CE91-0008 / FWF I 6159-N) and the ANR/DIADEM MIAM project (ANR-23-PEXD-0013).

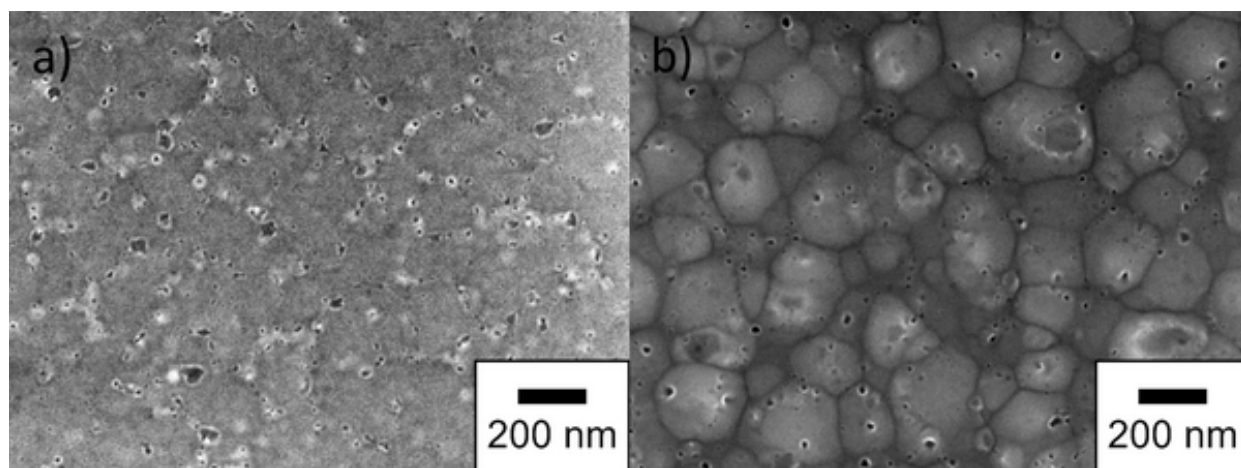


**Fig. 1:** Plane-view SEM images of the top surface of a NdFeB-based film, originally covered with a 10 nm thick Ta capping layer, after Ion Beam Etching for a) 10 min and b) 25 min (images are taken from different but neighbouring regions of the film). The contrast in the images originates from topographical differences and was obtained using a secondary electron detector.

📅 Mon. Jul 28, 2025 4:30 PM - 6:00 PM JST | Mon. Jul 28, 2025 7:30 AM - 9:00 AM UTC 🏠 Yellow zone, Conference rooms 101 and 102(1F)

## [P1] Processing, Characterization & Thin Films

Session Chair: Dr. Imants Dirba (Technical University of Darmstadt, Germany), Dr. Tae-Hoon Kim (Korea Institute of Materials Science, Korea)

### [P1-71] Characterization of rare earth garnet [Eu<sub>3</sub>Fe<sub>5</sub>O<sub>12</sub>/Tb<sub>3</sub>Fe<sub>5</sub>O<sub>12</sub>]/Gd<sub>3</sub>Ga<sub>5</sub>O<sub>12</sub> (111) ([EuIG/TbIG]/GGG (111)) thin films

\*Ko-Wei Lin<sup>1</sup>, Guan-Hua Lu<sup>1</sup>, Tai-Yi Chiu<sup>1</sup>, Chi Wah Leung<sup>2</sup> (1. National Chung Hsing University (Taiwan), 2. The Hong Kong Polytechnic University (China))

Keywords : rare-earth ion garnets thin films

The rare-earth ion garnets (ReIG) thin films have been studied recently due to potential applications in spintronics [1]. The hysteresis behavior was found in ReIG thin films with perpendicular magnetic anisotropy (PMA) through the anomalous Hall effect resistance (RAHE) of the ferromagnetic/heavy metal (FMI/HM) system. We have shown in our previous works where first, the advanced technology for example polarized neutron reflectometry (PNR) was used to study the magnetic proximity behavior at interfaces of Pt/TbIG/GGG (111) thin films [2]. Second, the tunable compensation temperature ( $T_{\text{comp}}$ ) was achieved in the Pt/EuIG/TbIG/GGG (111) thin film system with different EuIG thicknesses [3]. To this end, microstructures and chemical composition and/or oxidation states of the ReIG thin films play important roles in affecting the respected magnetic properties. In this study, microstructures and oxidation states of the EuIG/TbIG/GGG (111) thin film using PLD technique were investigated. Results obtained by field-emission transmission electron microscopy (FE-TEM) indicate that an epitaxial growth (with an in-plane compressive strain) was found in a EuIG(20 nm)/TbIG(30 nm) thin film deposited on GGG (111) single crystal substrates, in agreement with those characterized by XRD. In addition, results characterized by X-ray photoelectron spectroscopy (XPS) indicate that the EuIG/TbIG thin film consisted of Eu<sup>3+</sup> and Tb<sup>3+</sup> in the EuIG and TbIG layer, respectively. The peak shift as well as peak intensity variations in the Fe spectra imply that the changes in Fe valence and oxygen vacancies may be presence in the EuIG/TbIG thin film. Research was supported by NSC, Taiwan and Hong Kong Research Grants Council.

[1] E. R. Rosenberg et al., Phys. Rev. Mater 2, 094405 (2018).

[2] R. Yadav et al., Phys. Rev. Mater 7, 124407 (2023).

[3] P. G. Li et al., J. Magn. Magn. Mater 592, 171785 (2024).

📅 Mon. Jul 28, 2025 4:30 PM - 6:00 PM JST | Mon. Jul 28, 2025 7:30 AM - 9:00 AM UTC 🏠 Yellow zone, Conference rooms 101 and 102(1F)

## [P1] Processing, Characterization & Thin Films

Session Chair: Dr. Imants Dirba (Technical University of Darmstadt, Germany), Dr. Tae-Hoon Kim (Korea Institute of Materials Science, Korea)

### [P1-73] Effect of Ir addition on the crystal structure and magnetic properties for Mn-Ga thin films

\*Yuto Yamazaki<sup>1</sup>, Masaaki Doi<sup>1</sup>, Toshiyuki Shima<sup>1</sup> (1. Tohoku Gakuin University (Japan))

Keywords : Mn-Ga alloy、Ir addition、magneto-crystalline anisotropy、coercivity、thin film

High perpendicular magnetic anisotropy is required in spintronics devices, and among ferromagnetic alloys, MnGa alloy films are considered a promising material as they fully satisfy this requirement [1]. Recently, the detailed effects of magneto-crystalline anisotropy in Mn-Ga alloys have been reported using first-principles calculations, and it has been shown that the addition of small amount of Ir can significantly improve the magneto-crystalline anisotropy of Mn-Ga alloys [2]. In this study, Mn-Ga alloy thin films with varying amount of Mn and Ir were prepared to improve the magneto-crystalline anisotropy, and their crystal structure and magnetic properties were investigated in detail. All samples were prepared on MgO (100) single-crystal substrates using an ultra-highvacuum magnetron sputtering system. The base pressure of the deposition chamber was approximately  $5.0 \times 10^{-8}$  Pa and Ar gas was maintained at a pressure of 0.135 Pa during the sputtering process. Before deposition, the substrate was heated at 600°C for 30 minutes for cleaning, followed by the deposition of 70 nm of Ir-doped Mn-Ga thin film at 500°C. The amount of Mn in the Mn-Ga alloy was varied between 49.7 and 64.9 at.%. After deposition, the substrate was cooled down to room temperature and capped with a 10 nm thick Cr layer to prevent oxidization. The crystal structure was determined using an X-ray diffractometer (XRD), and the magnetic properties were evaluated using a superconducting quantum interference device (SQUID) magnetometer. From the XRD patterns, the (001) and (002) peaks of the  $L1_0$  structure were clearly observed when the Mn content was 49.7 at.%, and the (002) and (004) peaks of the  $D0_{22}$  structure were clearly observed between 53.8 and 64.9 at.%. When Ir was added to the Mn-Ga alloy thin films, their main peak positions shifted to the high-angle side in the case of compositions showing the  $L1_0$  structure and to the low-angle side in the case of composition regions showing the  $D0_{22}$  structure, and the intensity of their peaks was also reduced. The magnetization curves show that the addition of Ir decreases the saturation magnetization of the Mn-Ga thin film both in-plane and perpendicular direction to the film plane, while the coercive force increases. In the  $Mn_{59.9}Ga_{40.1}$  thin film sample, the magneto-crystalline anisotropy increased when the amount of Ir was 4.0 at.%, confirming that the coercive force and magneto-crystalline anisotropy of the Mn-Ga thin film were improved by Ir addition.

#### References

1) Yumei Zhang, Wen Zhang, Mengyao Ning, Lingli Chen, Haibo Li, *Sur. Sci.*, **542**, 148585

(2021).

2) Lukas Wollmann, Stanislav Chadov, Jürgen Kübler, and Claudia Felser, *Rev. B*, **92**, 064417 (2015).

📅 Mon. Jul 28, 2025 4:30 PM - 6:00 PM JST | Mon. Jul 28, 2025 7:30 AM - 9:00 AM UTC 🏠 Yellow zone, Conference rooms 101 and 102(1F)

## [P1] Processing, Characterization & Thin Films

Session Chair: Dr. Imants Dirba (Technical University of Darmstadt, Germany), Dr. Tae-Hoon Kim (Korea Institute of Materials Science, Korea)

### [P1-74] Magnetocaloric effect of textured polycrystalline $\text{RNi}_5$ alloys

\*Iurii Koshkidko<sup>1</sup>, Jacek Ćwik<sup>1</sup> (1. Institute of Low Temperature and Structure Research, PAS, Okólna 2, Wrocław, 50-422 (Poland))

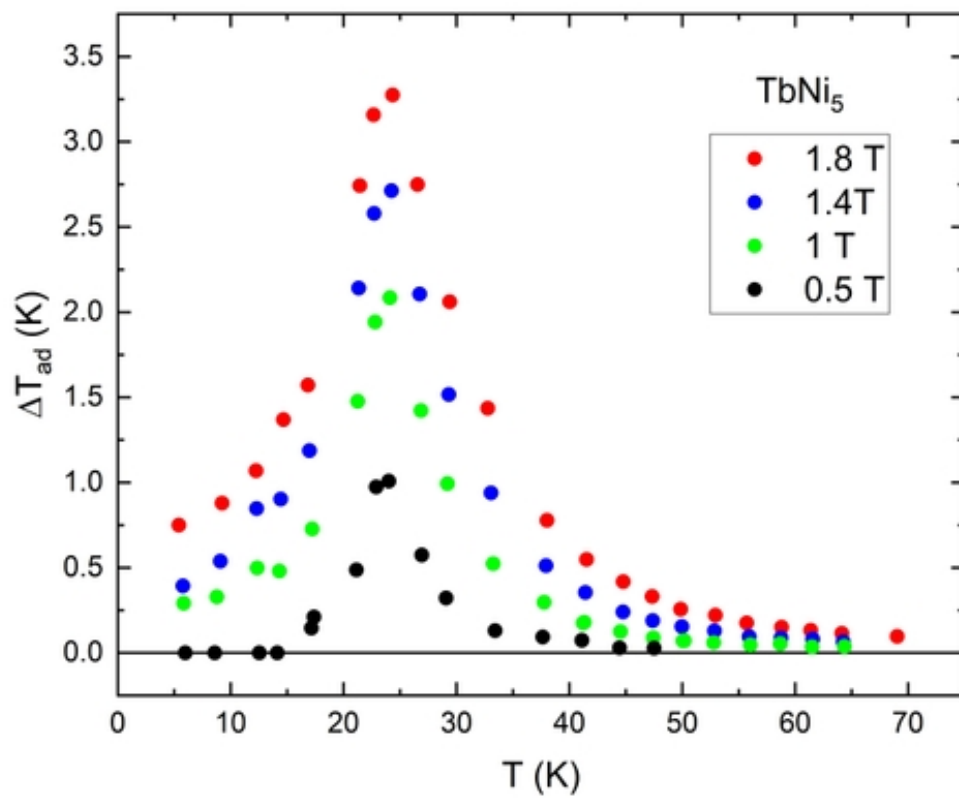
Keywords : Magnetocaloric effect, Magnetic phase transition, Magnetocrystalline anisotropy, Intermetallic compounds, Rare earth metals

The study of the magnetocaloric effect (MCE) is relevant for application in energy-saving magnetic refrigeration technology (MRT). The application of MRT in the low-temperature region can contribute to increasing the efficiency of manufacturing and application of liquid gases (e.g. helium, hydrogen, nitrogen, natural gases, etc.), and will also reduce losses associated with their transportation and storage. It is known that the physics of magnetic phenomena consider two main types of MCE. The first one is the MCE of paraprocess, i.e., MCE related to the process of ordering magnetic moments during magnetization of a magnetic material in a magnetic field, which were disordered as a result of thermal fluctuations [1]. The second type is the rotating (anisotropic) MCE (RMCE) caused by the magnetization rotation as a result of the magnetization of the magnetic materials along the hard magnetization axis of the magnetic materials. The MCE of paraprocess is fairly well studied, while the RMCE remains rather poorly understood. First of all, this is related to difficulties in creating samples and methods for such investigations. In [2], it was theoretically shown that the RMCE values for  $\text{RNi}_5$  compound can reach the giant value  $\Delta T_{\text{ad}} = 5.5$  K in a field of 1 T at a temperature of 7 K for  $\text{ErNi}_5$ . For comparison, the previously experimentally observed giant rotating MCE in the region of spin-reorientation transition in  $\text{NdCo}_5$  single crystal was  $\Delta T_{\text{ad}} = 1.6$  K in a field of 1.3 T at a temperature of 278 K [3].

The authors of works [2] highlight that experimental data on the anisotropic MCE for  $\text{RNi}_5$  are still absent. Intermetallic compounds  $\text{RNi}_5$  are excellent model objects for studying the mechanisms of formation of magnetic properties in 4f and 3d-metal compounds. They have a hexagonal structure of the  $\text{CaCu}_5$  type. The 3d-band of Ni is practically occupied by the external electrons of R atoms. As a consequence, the Ni atoms do not contribute significantly to the spontaneous magnetic moments of  $\text{RNi}_5$ . Therefore,  $\text{RNi}_5$  with non-magnetic  $\text{R}=\text{La}, \text{Ce}, \text{Lu}$  or  $\text{Y}$  are Pauli paramagnetics.  $\text{RNi}_5$  compounds with magnetic  $\text{R}=\text{Nd}, \text{Sm}, \text{Gd}, \text{Tb}, \text{Dy}, \text{Ho}$  and  $\text{Er}$  are ferromagnets with Curie  $T_{\text{C}}$  temperatures lying below 32 K. In turn, strong magnetocrystalline anisotropy (MCA) is observed in  $\text{RNi}_5$  compounds with magnetic R. For  $\text{R}=\text{Sm}, \text{Er}, \text{Tm}$ , the “easy axis” type of MCA is characteristic, and for  $\text{R}=\text{Pr}, \text{Nd}, \text{Tb}, \text{Dy}, \text{Ho}$  “easy plane” [4]. Recently, polycrystalline magnetocaloric materials with RMCE have attracted more attention due to their more convenient sample preparation than monocrystalline materials [5]. The induced magnetic anisotropy in such



materials is realised by texturing magnetic powder in a strong magnon field followed by fixation in a non-magnetic matrix or by directed crystallisation. The latter method was used in this work to create polycrystalline samples of  $\text{RNi}_5$  with induced magnetic anisotropy. Polycrystalline alloy  $\text{RNi}_5$  was synthesised by arc melting of the elements in a purified argon atmosphere in a water-cooled copper crucible. The arc-melted ingot was inverted and remelted four times to ensure homogeneity. Microstructures were observed using a scanning electron microscope and grain orientation was investigated using electron backscattered electron diffraction (EBSD). To investigate MCE in medium magnetic fields (up to 1.8 T), we used a magnetic field source based on permanent magnets (produced by AMT&C) and an apparatus for direct MCE measurements placed on a rotary table [6]. This allowed measurements in different directions relative to the main axis of the magnetic texture of the sample. This method is of particular interest because the magnitude of the magnetic field corresponds to that to be used in magnetic refrigeration systems. In this work we present the results of the MCE study by direct method of synthesised polycrystalline  $\text{RNi}_5$  with induced magnetic anisotropy (See Fig.). The influence of magnetocrystalline anisotropy on the magnitude of RMCE is discussed. The work was supported by the National Science Center, Poland through the OPUS Program under Grant No. 2024/53/B/ST11/02445. [1] Tishin A.M., Spichkin Y.I., "The magnetocaloric effect and its applications", Institute of Physics Publishing, Bristol, Philadelphia, 2003, 475 p. [2] N.A. de Oliveira, Journal of Physics and Chemistry of Solids 103 (2017) 13–15 [3] Nikitin, S., Skokov, K., Koshkid'ko, Yu., Pastushenkov, Yu., Ivanova, T., PRL 105 (2010) 137205 [4] W.E. Wallace, Rare-Earth Intermetallics, Academic Press, New York, London (1973) p. 266. [5] Xiaoyu Zhou, et al., Appl. Phys. Lett. 120, 132401 (2022) [6] Koshkid'ko, Y.S., Ćwik, J., Ivanova, T.I., Nikitin, S.A., Miller, M., Rogacki, K., JMMM 433 (2017) 234



📅 Mon. Jul 28, 2025 4:30 PM - 6:00 PM JST | Mon. Jul 28, 2025 7:30 AM - 9:00 AM UTC 🏠 Yellow zone, Conference rooms 101 and 102(1F)

## [P1] Processing, Characterization & Thin Films

Session Chair: Dr. Imants Dirba (Technical University of Darmstadt, Germany), Dr. Tae-Hoon Kim (Korea Institute of Materials Science, Korea)

### [P1-75] The influence of phosphorization treatment on the high-temperature oxidation resistance of Nd-Fe-B magnetic powder

\* Jingwu Zheng<sup>1</sup>, Xinqi Zhang<sup>1</sup>, Dongsheng Shi<sup>1</sup>, Wei Cai<sup>1</sup>, Liang Qiao<sup>1</sup>, Yao Ying<sup>1</sup>, Shenglei Che<sup>1</sup> (1. Research Center of Magnetic and Electronic Materials, College of Materials Science and Engineering, Zhejiang University of Technology, Hangzhou 310014, China (China))

Keywords : Nd-Fe-B powders、Anti-oxidation、phosphorylation、Methylene diphosphonic acid (MDPA)

The commonly employed industrial approach for enhancing the high-temperature oxidation resistance of rare earth magnetic powder involves conducting surface phosphating treatment to generate a phosphate conversion coating. In response to the environmental concerns associated with the utilization of high-concentration inorganic phosphoric acid as a surface modifier, this article introduces a sustainable alternative in the form of a green organic phosphonic acid modifier (Methylene diphosphonic acid, MDPA). Furthermore, the impact of treatment with inorganic phosphoric acid and MDPA on the magnetic properties and antioxidant performance is investigated. The results indicate that, compared to the untreated powder, the coercivity and maximum magnetic energy product of the magnetic powder exhibit a slight decrease after treatment with inorganic phosphoric acid and MDPA at room temperature. However, there is a significant improvement in the high-temperature oxidation resistance of the magnetic powder. Moreover, MDPA demonstrates a superior modification effect compared to inorganic phosphoric acid. The enhanced magnetic performance at elevated temperatures following phosphating treatment can be attributed to the formation of a conversion coating characterized by uniformity and density, primarily composed of metal phosphates. After treatment with inorganic phosphoric acid, the conversion film exhibits a relatively higher Nd content. This phenomenon can be attributed to the preferential corrosion of the intergranular Nd-rich phase of magnetic powder by inorganic phosphoric acid, while the conversion film formed through MDPA treatment primarily consists of iron phosphate, resulting in a comparatively lower Nd content. This observation may provide an explanation for the lesser impact on magnetic performance with MDPA treatment.



# The influence of phosphorization treatment on the high-temperature oxidation resistance of Nd-Fe-B magnetic powder

Jingwu Zheng\*, Xinqi Zhang, Dongsheng Shi, Wei Cai, Liang Qiao, Yao Ying, Shenglei Che\*

Research Center of Magnetic and Electronic Materials, College of Materials Science and Engineering, Zhejiang University of Technology, Hangzhou 310014, China

Background

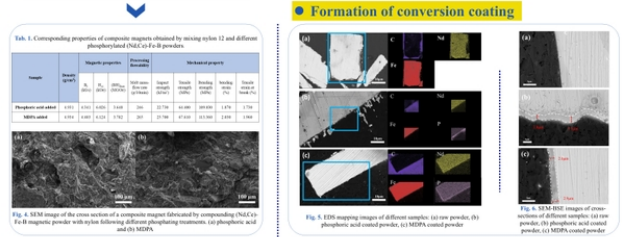
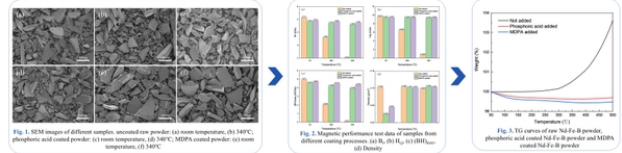
- Nd-Fe-B permanent magnets are widely used in electric vehicles and other fields, but are prone to oxidation at high temperatures, leading to a decline in magnetic performance
- Improving the high-temperature oxidation resistance of magnetic powders is a key challenge for ensuring long-term stability and performance
- The traditional use of high-concentration inorganic phosphoric acid for surface phosphating causes environmental pollution, creating an urgent need for green alternatives

Objective

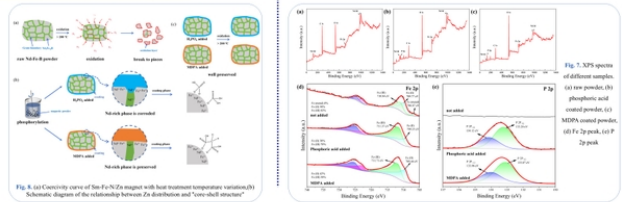
- A comparison of the effects of inorganic phosphoric acid and organic phosphonic acid (MDPA) on the high-temperature oxidation resistance and performance of powders
- Exploring the differences between MDPA treatment and traditional inorganic phosphoric acid treatment in enhancing high-temperature oxidation resistance

Results and discussion

Oxidation Resistance Properties



Mechanism of modification



Conclusion

- MDPA treatment significantly enhances the high-temperature oxidation resistance of Nd-Fe-B magnetic powders, with only a slight decrease in magnetic performance.
- Compared to inorganic phosphoric acid, MDPA treatment shows superior modification effects in high-temperature oxidation environments.
- The MDPA conversion film is primarily composed of iron phosphate, which reduces Nd corrosion, improves interface compatibility with nylon, and supports large-scale production